

INVESTIGATION OF NLRP13'S CLEAVAGE AND ITS ROLE IN
MACROPHAGE POLARIZATION

by

Sevgi ıracı

B.S., Molecular Biology and Genetics, Boğaziçi University, 2020

Submitted to the Institute for Graduate Studies in
Science and Engineering in partial fulfillment of
the requirements for the degree of
Master of Science

Graduate Program in Molecular Biology and Genetics
Boğaziçi University

2022

ACKNOWLEDGEMENTS

Firstly, I would like to thank my supervisor Prof. Nesrin Özören for giving me the opportunity to conduct this work and also for her supervision and guidance over the years. I am thankful to my thesis committee members Prof. Güneş Esendağlı and Assoc. Prof. Tolga Sütü for taking the time to evaluate my thesis.

I would like to thank the most outstanding team members ever: İlke Süder, Hafize Özen Kaya, Davod Khalafkhany, Efe Elbeyli, Hilal Ok, Elif Öykü Çakır, Dilvin Berrak Güney and our intern İrem Ceren for always being helpful, supportive, cooperative and for having this incredible matchless energy.

I would like to mention my favorite things about my teammates. I love how İlke can be selfless when someone is in need at the laboratory, and I am proud to stay as the person she supervised the most, starting from my intern, baby, times, even if she has her own lab team, I was there before them. Özen is my lost older sister, she never stops thinking about you if you have the smallest problem, I was lucky to have her around for my dummiest questions to be answered without being judged, and it's always better to be with her regardless of us laughing or crying together. Davod is the older brother who has solutions to everything, he makes life easier for everyone, and I love how he observes and realizes that you're not feeling well before anyone else, and is always there for you. Efe boosts the mood anytime but also is a friend in need, and never thinks twice if you ask for something. I loved working and being goofy around with the other two members of team NLRP13, Hilal and Öykü. Hilal saved me on many points during this project, she is the person you can always count on anything, and she is my favorite person to annoy since she's so sweet. Öykü lessened my burden for this project and I love that she makes me feel less lonely by joining me in my stupid, funny times, also I was happy to be Eddie and Crush to people with her. İrem came at the last moment but quickly became one of us and helped me a lot. They were there for me at my 3 am brainstorming sessions or 3 pm breakdowns. They made life better, they made me a better version of myself and I am the happiest that I have spent 4

years with them.

I would like to thank Assoc. Prof. Stefan Fuss for teaching me confocal microscopy.

I am thankful to Elif Çelik for teaching me and aiding me in flow cytometry and FACS. I also thank Ulduz Sophia Afshar, M. Sc., for always being open to my questions and helping me on many points in this project. Additionally, thanks to Zeynep Dokuzluoğlu, I could analyze and show my data better with Image J and Adobe Illustrator. I am thankful to many people in the department for being so friendly, sweet, and helpful.

Additionally, I would like to thank Sütü Lab, MTCRL (Yaman Lab), and Sumo Lab for providing the needed materials and equipment used in the experiments carried out for this thesis.

Special thanks to my dear friends Anastasiya Yılmaz (my unofficial academic consultant), Habibe Nur Koyuncu, Tuğçe Uysal, Tolga Gürcan, Mehmet Yılmaz, also Elif Aysu Solak, İrem Yıldız, İrem Öztaş, Büşra Süzer, Şenay Uzuner, Tuğba Ecem Sakallı, and MX (OT7) for always being there for me.

I want to thank my family Elif Çıracı, Akın Çıracı, Erdem Çıracı for their endless support. And, I want to thank myself the most for getting through this master's.

ABSTRACT

INVESTIGATION OF NLRP13'S CLEAVAGE AND ITS ROLE IN MACROPHAGE POLARIZATION

The NOD-like receptors (NLRs) are mainly known for their roles in inflammatory responses and host defense against microbial pathogens, but they are also associated with metabolic disorders, autophagy regulation, transcription regulation, early embryogenesis, reproduction, and yet unknown functions. Several NLRs have been demonstrated to assemble inflammasomes which are cytosolic multiprotein complexes that can induce pyroptosis. NLRP13 is a PYRIN containing NLR protein that is found in non-rodents. There is little to no information about NLRP13 in the literature. It is determined that NLRP13 is involved in inflammasome formation and cleaved forms of this protein can be found in the cell, by the former students of our lab. In my thesis project, NLRP13's cleavage and its possible involvement in macrophage polarization were investigated. We showed that the C-terminal of NLRP13 protein colocalizes with mitochondria after being cleaved by Caspase-8 in an overexpression model utilizing immunofluorescence and visualization by confocal microscopy. It was indicated that NLRP13 does not participate in intracellular endosomal trafficking. Additionally, it was suspected that NLRP13 might be involved in macrophage polarization. For this, THP-1 monocytes were differentiated into M1 and M2 macrophages to be analyzed by RT-qPCR and flow cytometry. No difference was observed for wild-type, plasmid control, and NLRP13 overexpressing THP-1 macrophages. Overall, the localization of cleaved forms of NLRP13 *in vitro* was determined and it was shown that NLRP13 has no role in macrophage polarization in THP1.

ÖZET

NLRP13'ÜN KESİLİMİNİN VE MAKROFAJ POLARİZASYONUNDAKİ MUHTEMEL GÖREVİNİN ARAŞTIRILMASI

NOD benzeri reseptörler (NLR'ler) temel olarak inflamatuvar yanıtlardaki rolleri ve mikrobiyal patojenlere karşı konak savunmasındaki rolleri ile bilinirler, ancak aynı zamanda metabolik bozukluklar, otofaji regülasyonu, transkripsiyon regülasyonu, erken embriyogenez, üreme ve benzeri roller ile de ilişkilidirler. NLRP13, PYRIN bölgesi bulunduran bir NLR proteindir ve kemirgen olmayanlarda bulunur. Literatürde NLRP13 hakkında neredeyse hiç bilgi bulunmamaktadır. NLRP13'ün iltihaplanma oluşumunda rol oynadığı ve bu proteinin kesilmiş formlarının hücrede bulunabileceği laboratuvarımızın eski öğrencileri tarafından belirlendi. Bu proje boyunca, bölünmesi ve makrofaj polarizasyonuna olası katılımı araştırıldı. NLRP13 proteininin C-terminalinin, immünofloresan ve konfokal mikroskopisi ile aşırı ifade modelinde Caspase-8 tarafından parçalandıktan sonra mitokondride bulunduğunu gösterdik. NLRP13'ün hücre içi endozomal trafiğe katılmadığı belirlendi. Ek olarak, NLRP13'ün makrofaj polarizasyonuna dahil olabileceğinden şüpheleniliyordu. Bunun için THP-1 monositleri M1 ve M2 makrofajlarına farklılaştırıldı, daha sonra RT- qPCR ve akış sitometrisi ile analiz edildi. Yabancı tip, plazmit kontrolü ve NLRP13'ü aşırı ifade eden THP-1 makrofajları için hiçbir fark gözlenmedi. Genel olarak, NLRP13'ün kesilmiş formlarının lokalizasyonu *in vitro* olarak belirlendi ve NLRP13'ün THP1'de makrofaj polarizasyonunda rolü olmayabileceği gösterildi.

TABLE OF CONTENTS

ACKNOWLEDGEMENTS	iii
ABSTRACT	v
ÖZET	vi
LIST OF FIGURES	x
LIST OF TABLES	xiii
LIST OF SYMBOLS	xv
LIST OF ACRONYMS/ABBREVIATIONS	xvi
1. INTRODUCTION	1
1.1. Adaptive and Innate Immune Systems	1
1.2. Pattern Recognition Receptors	2
1.3. NOD-Like Receptors	3
1.4. Inflammasomes	5
1.5. NLRP13	6
1.6. Caspases	8
1.7. Caspase 8	9
1.8. Macrophage Polarization	10
2. HYPOTHESIS AND PURPOSE	11
3. MATERIALS	12
3.1. Cell Lines	12
3.1.1. Human Embryonic Kidney Cell Line (HEK293FT)	12
3.1.2. THP1 Monocytic Cell Line	12
3.2. Chemicals, Plastics and Glassware	12
3.3. Buffers and Solutions	13
3.3.1. Cell Culture	13
3.3.2. Molecular Cloning	14
3.3.3. Transfection and Transduction.	14
3.3.4. Western Blotting	15
3.3.5. Culture of Bacteria	17
3.4. Fine Chemicals	18

3.4.1.	Plasmids	18
3.4.2.	Primers	19
3.4.3.	Oligos	19
3.4.4.	Antibodies	20
3.5.	Kits	20
3.5.1.	Kits	20
3.6.	Equipments	21
3.6.1.	Equipments	21
4.	METHODS	23
4.1.	Cell Culture	23
4.1.1.	Maintenance of Cells	23
4.1.2.	Calcium Phosphate Transfection of HEK293FT	24
4.1.3.	Transduction of THP1 Cells	24
4.2.	Gene Expression Analysis	24
4.2.1.	RNA Isolation	24
4.2.2.	cDNA Synthesis	25
4.2.3.	RT-qPCR	25
4.3.	Western Blotting	26
4.4.	Macrophage Polarization Assay	27
4.5.	Flow Cytometry	27
4.6.	Cleavage of NLRP13	28
4.6.1.	Competent Cell Preparation	28
4.6.2.	Transformation	28
4.6.3.	Plasmid Isolation	29
4.6.4.	Restriction Enzyme Digestion	29
4.6.5.	Polymerase Chain Reaction	29
4.6.6.	Agarose Gel Electrophoresis	31
4.7.	Statistical Analysis	31
5.	RESULTS	32
5.1.	Cleavage of NLRP13	32
5.1.1.	Cloning of HA-tag to NLRP13-FLAG	32
5.1.2.	Activation of Caspase-8	35

5.1.3. Immunofluorescence of NLRP13 Cleavage	37
5.2. Macrophage Polarization	42
5.2.1. Optimization of Macrophage Polarization Assay	42
5.2.2. Visualization of Macrophage Polarization Assay	43
5.2.3. NLRP13 Expression of Different Macrophage Subsets	45
5.2.4. mRNA Expression of Macrophage Polarization Assay	46
5.2.5. Cell Surface Marker Expression of Macrophage Polarization Assay	47
5.3. Knockdown of NLRP13 in THP-1 Cells via CRISPR/CAS9 Technology	49
6. DISCUSSION	55
REFERENCES	60
APPENDIX A: PLASMID MAPS	65

LIST OF FIGURES

Figure 1.1.	Classification of the NLR gene family.	4
Figure 5.1.	Agarose gel confirmation of the PCR product.	33
Figure 5.2.	Verification of recombinant FLAG-NLRP13-HA plasmid via double digestion.	34
Figure 5.3.	Confirmation of HA and FLAG protein expression via SDS-PAGE Western Blotting following the HEK293FT transfection of the plasmids obtained from the picked colonies.	35
Figure 5.4.	Caspase-8 activity upon CD95 treatment trial via SDS-PAGE Western Blotting.	36
Figure 5.5.	NLRP13 cleavage upon CD95 treatment trial.	37
Figure 5.6.	Colocalization of Rab5 with HA-tag and FLAG-tag of NLRP13.	38
Figure 5.7.	Colocalization of Rab9 with HA-tag and FLAG-tag of NLRP13.	39
Figure 5.8.	Colocalization of Rab11 with HA-tag and FLAG-tag of NLRP13.	39
Figure 5.9.	Colocalization of MTS-DsRED with HA and FLAG tags of NLRP13.	41
Figure 5.10.	Quantification of colocalization of MTS-DsRED with HA-tag and FLAG-tag of NLRP13 via Image J.	42
Figure 5.11.	Optimization of macrophage polarization assay using RT-qPCR.	43

Figure 5.12. WT, mCherry and NLRP13 overexpressed THP1 nontreated monocytes and macrophages after 24 hours PMA treatment.	44
Figure 5.13. WT, mCherry and NLRP13 overexpressed THP1 M0, M1 and M1 macrophages.	45
Figure 5.14. The expression of NLRP13 in monocytes, M0, M1 and M2 macrophages.	46
Figure 5.15. The mRNA expression of M1 marker, CD80, and M2 marker, CD206, in monocytes, M0, M1 and M2 macrophages of WT, mCherry and NLRP13 THP1.	47
Figure 5.16. CD80 cell surface marker expression in monocytes, M0, M1 and M2 macrophages of WT, mCherry and NLRP13 THP1.	48
Figure 5.17. CD206 cell surface marker expression in monocytes, M0, M1 and M2 macrophages of WT, mCherry and NLRP13 THP1.	48
Figure 5.18. Transfection efficiency of HEK293FT cells transfected with sgRNA plasmids along with the packaging plasmids.	49
Figure 5.19. Transduction efficiency of lentiviral guide RNA containing viruses.	50
Figure 5.20. GFP Positivity after sorting according to GFP positivity and selecting via puromycin.	51
Figure 5.21. Protein expression of Cas9 upon dox induction.	52
Figure 5.22. The expression of NLRP13 in guide RNA containing THP1 cells after dox induction.	52

Figure 5.23. Agarose gel visualization of PCR amplification of the regions targeted by guide RNAs.	53
Figure 5.24. NLRP13 protein expression upon LPS/ATP treatment in guide RNA containing THP1 macrophages.	54
Figure 6.1. Updated model of NLRP13.	59
Figure A.1. Map of pcDNA3-NLRP13-FLAG vector.	65
Figure A.2. Map of the pLKO5.sgRNA.EFS.GFP vector.	66

LIST OF TABLES

Table 3.1.	Cell culture chemicals.	13
Table 3.2.	Enzymes used in cloning.	14
Table 3.3.	Transfection and transduction reagents.	14
Table 3.4.	Chemicals used in SDS-PAGE gel preparation.	15
Table 3.5.	Solutions used in Western Blotting.	16
Table 3.6.	Chemicals used in Western Blotting.	17
Table 3.7.	Chemicals used in culture of bacteria.	17
Table 3.8.	Plasmids.	18
Table 3.9.	Primers used in RT-qPCR and Sanger sequencing.	19
Table 3.10.	Oligos used in cloning.	19
Table 3.11.	Antibodies.	20
Table 3.12.	Kits.	20
Table 3.13.	Equipments I.	21
Table 3.14.	Equipments II.	22
Table 4.1.	RT-qPCR components.	26

Table 4.2.	qPCR conditions.	26
Table 4.3.	First PCR components.	29
Table 4.4.	First PCR conditions.	30
Table 4.5.	Second PCR components.	30
Table 4.6.	Second PCR conditions.	31

LIST OF SYMBOLS

°C	Degree Celcius
g	Gram
g	Gravity
h	Hour
kDa	Kilodalton
L	Liter
M	Molar
mg	Miligram
mM	Milimolar
mm	Milimeter
ml	Mililiter
min	Minute
ng	Nanogram
rpm	Revolutions per Minute
sec	Second
V	Volt
α	Alpha
β	Beta
γ	Gamma
δ	Delta
κ	Kappa
μg	Microgram
μM	Micromolar
μl	Microliter

LIST OF ACRONYMS/ABBREVIATIONS

Ab	Antibody
AD	Acidic Transactivation Domain
ALRs	Absent in melanoma 2 (AIM2)-like receptors
APS	Ammonium Persulfate
ASC	Apoptosis Associated Speck-Like Protein Containing CARD
ATP	Adenosine Triphosphate
BIR	Baculoviral Inhibitory Repeat-like Domain
BSA	Bovine Serum Albumin
CARD	Caspase Activation and Recruitment Domain
CAS9	CRISPR Associated Protein 9
Caspase	Cysteine-Aspartic Protease
cDNA	Complementary DNA
CLR	C-type Lectin Receptor
CRISPRi	Clustered Regularly Interspaced Short Palindromic Repeats Interference
DAMP	Danger Associated Molecular Patterns
DC	Dendritic Cell
dH ₂ O	Distilled water
ddH ₂ O	Double-distilled water
DISC	Death-Inducing Signaling Complex
DMEM	Dulbecco's Modified Eagle Medium
DMSO	Dimethyl Sulfoxide
DNA	Deoxyribonucleic Acid
EDTA	Ethylenediaminetetraacetic Acid
EGFP	Enhanced Green Florescent Protein
FADD	Fas-associated Protein with Death Domain
FBS	Fetal Bovine Serum
FC	Flow Cytometry
GFP	Green Fluorescence Protein

HBS	Hepes Buffer Saline
HEK293	Human Embryonic Kidney Cells
IFN	Interferon
IL	Interleukin
LB	Luria Broth
LRR	Leucin Reach Repeat
LPS	Lipopolysaccharide
MAVS	Mitochondrial Antiviral Signaling Protein
MHC	Major Histocompatibility Complex
mRNA	Messenger RNA
NACHT	Present in NAIP, CIITA, HET-E, and TP1
NaCl	Sodium Chloride
NEAA	Non-essential Amino Acid
NLR	NOD-Like Receptor
NOD	Nucleotide-binding Oligamerization Domain
OD	Optical Density
PAMP	Pathogen Associated Molecular Pattern
PBS	Phosphate Buffer Saline
PBS-T	Phosphate Buffer Saline and Tween 20
PCR	Polymerase Chain Reaction
PFA	Paraformaldehyde
PMA	Phorbol 12-Myristate 13-Acetate
PRR	Pattern Recognition Receptor
PVDF	Polyvinylidene fluoride
PYD	Pyrin Domain
RLR	RIG-I-like Receptor
RNA	Ribonucleic Acid
ROS	Reactive Oxygen Species
RT	Room Temperature
RT-PCR	Reverse Trascriptase PCR
qPCR	Quantitative PCR

SDS	Sodium Dodecyl Sulfate
SDS-PAGE	SDS-Polyacrylamide Gel Electrophoresis
sgRNA	Single Guide RNA
TBS	Tris Buffered Saline
TBS-T	Tris Buffered Saline and Tween 20
TEMED	N,N,N',N'-Tetramethyl ethylenediamine
TLR	Toll Like Receptor
TNF	Tumor Necrosis Factor
Tween 20	Polysorbate
v	Volume
w	Weight
WB	Western Blot
WT	Wild Type

1. INTRODUCTION

1.1. Adaptive and Innate Immune Systems

All organisms need to defend themselves against pathogens. While the invertebrates protect themselves via strategies such as restriction factors and protective barriers, vertebrates have their immune system, which is divided into the innate and adaptive immune systems. The innate immune system gives the initial response to eliminate the invaders with general strategies, and in the case of a pathogen still persists despite the first line of defense by the innate immune system, innate immune system elements recruit the adaptive immune system response, of which is highly specified to the pathogen. Unlike the innate immune responses, adaptive immune responses are lasting and preserve the memory of the infection to react faster in the case of encountering the same infection in the future. These two systems have different mechanisms to detect, differentiate and eliminate pathogens. The mechanism of the innate immune system is composed of sensors that recognize the distinct patterns which are unknown or possibly belong to a pathogen. The adaptive immune system produces countless types of proteins specific to the unfamiliar molecules to identify them, such as T and B cell receptors and antibodies. (Alberts, 2015)

The pathogens face two kinds of defense with the innate immune system. First, physical and chemical barriers set an overall barrier against the invader with the components such as the skin, mucosal tissue, pH and complement system, and so on. Second, the innate immune cells respond. These cells are composed of monocytes, macrophages, neutrophils, dendritic cells (DC), natural killer (NK) cells, mast cells, eosinophils, and basophils. While the B and T cells are highly specific to the pathogen with their antigen recognition receptors, innate immune cells give a nonspecific response upon the encounter with the common molecular patterns, which are seen on the pathogens, and damaged or apoptotic cells through pattern recognition receptors. (Li and Wu, 2021)

1.2. Pattern Recognition Receptors

Pattern Recognition Receptors (PRRs) is a class of proteins that are specialized in the recognition of the molecular patterns frequently found on the surface of the pathogens and molecules released by the infected apoptotic and damaged senescent cells. These motifs can be named as Pathogen-Associated Molecular Patterns (PAMPs) or Damage-Associated Molecular Patterns (DAMPs), respectively. Following the engagement of PRRs with the ligands, pro-inflammatory and immunoprotective responses are initiated. (Li and Wu, 2021)

PRRs can be found as plasma membrane-bound, cytosolic, or intracellular compartment membrane-bound. They essentially contain ligand recognition domain, intermediate and effector domains, which allows them to recognize and bind to the PAMPs and DAMPs, recruit adaptor molecules and start the signal transduction to activate and release the necessary cytokines, chemokines, growth factors, and hormones. PRRs are classified into five groups which partly differ in their ligand recognition mechanisms, signaling pathways, and sub-cellular localization. They are named Toll-like receptors (TLRs), nucleotide oligomerization domain (NOD)-like receptors (NLRs), retinoic acid-inducible gene-I (RIG-I)-like receptors (RLRs), absent in melanoma-2 (AIM2)-like receptors (ALRs) and C-type lectin receptors (CLRs) according to their protein domain homology. (Li and Wu, 2021)

TLRs are transmembrane proteins that are found chiefly in the membrane or the endosomes. They recognize numerous exogenous and endogenous danger signals, which range from lipids, lipoproteins, and proteins to nucleic acids according to where they are located. NLRs are cytosolic sensors that consist of the nucleotide-binding domain (NBD or NACHT), leucine-rich repeats (LRRs), and effector domain that is either caspase activation and recruitment domain (CARD) or pyrin domain (PYD). They have multiple subfamilies and can recognize the bacterial, viral, and parasitic PAMPs within the cytosol. CLRs are expressed on the plasma membrane of phagocytic and antigen-presenting cells such as macrophages and dendritic cells (DCs), and they differentiate the carbohydrates of non-self-structures to initiate the signaling pathways

to control the infection. RLRs are cytoplasmic PRRs that recognize viral RNAs. ALRs are the sensors of cytosolic and nuclear pathogen DNA. (Li and Wu, 2021)

1.3. NOD-Like Receptors

The NOD-like Receptors (NLRs) are cytosolic pattern recognition receptors that sense the stress or injury within the intracellular environment. They are evolutionarily highly conserved and can be found among plant and animal kingdoms. (Zhong *et al.*, 2013). NLRs are characterized by including a central nucleotide-binding domain (NBD) that is a part of the NACHT domain and a C-terminal leucine-rich repeat (LRR) (Platnich and Muruve, 2019) (platnich). NACHT or NOD domain is involved in oligomerization, LRRs are necessary for ligand binding, and N-terminal is responsible for the homophilic protein-protein interaction (Zhong *et al.*, 2013)

There are 23 NLRs known in humans and more than 34 NLRs in mice (Franchi *et al.*, 2009). They are classified into four main subfamilies based on their N-terminal effector domain, which can be either one of the pyrin (PYD) domain, caspase recruitment domain (CARD), acidic transactivation domain (AD), baculoviral inhibitory repeat (BIR)-like domains (Ting *et al.*, 2008). Pyrin containing the NLRP subfamily includes 14 members, which are NLRP1-14. There are six members of the NLC family that has CARD or CARD-related X domain at their N-terminal, which are NOD1 (NLRC1), NOD2 (NLRC2), NLRC3, NLRC4, NLRC5, NLRX1. NLRA and NLRB subfamilies contain only one member each. NLRA subfamily has an AD domain and consists of class II major histocompatibility complex transactivator (CIITA). NLRB subfamily has a BIR domain, and its member is the NLR family apoptosis inhibitory protein (NAIP). (Liu *et al.*, 2019)

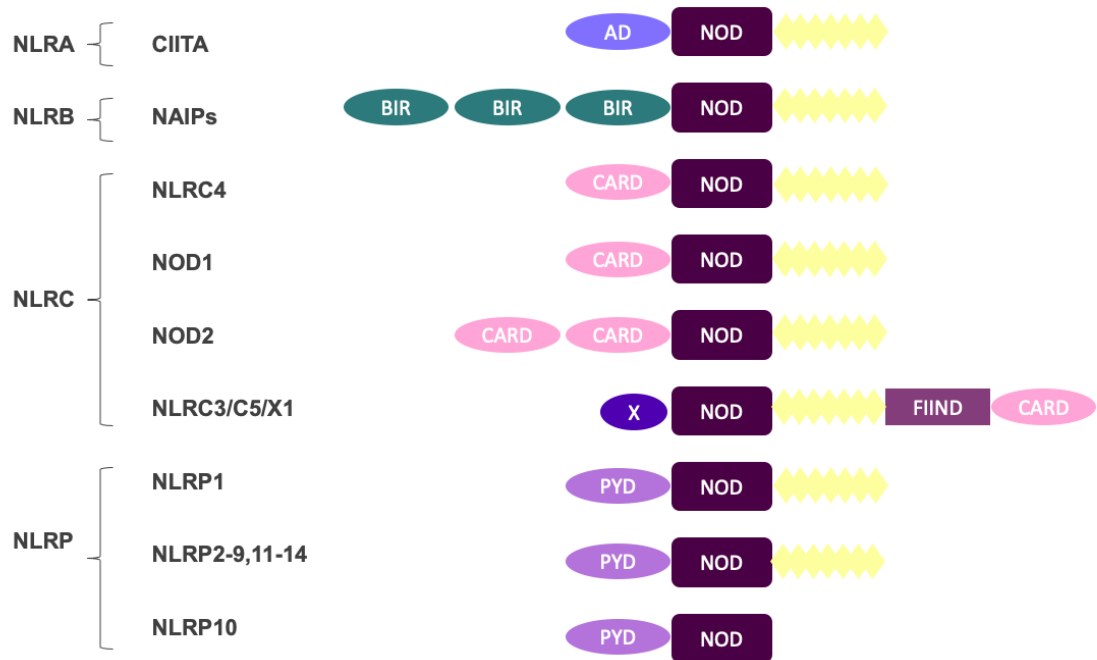


Figure 1.1. Classification of the NLR gene family (Adapted from Zhong *et al.*, 2013).

NLRs are highly conserved multidomain NTPases that activate the downstream pathways, which are related to immune responses, tumorigenesis, senescence, and stemness in response to the signal they receive. They are capable of recognizing a specific number of ligands from microbial pathogens, host cells, and environmental components. NOD1 and NOD2 sense the fragments of bacterial peptidoglycan, NLRC4 and NAIP recognize flagellin, and NLRP1 is activated as a response to the anthrax-lethal toxin and muramyl dipeptide. NLRP3 is activated through various ligands such as ATP, nigericin, uric acid crystals, and bacterial RNA. Upon the PAMP binding to the LRR region of NLRs, ADP/GDP is exchanged for ATP/GDP through conformational changes, which leads to the activation of downstream pathways. (Liu *et al.*, 2019)

NLRs involve in many roles ranging from autophagy, signal transduction, and transcription activation to inflammasome formation (Kim *et al.*, 2016). While NOD1, NOD2, NLRP10, NLRX1, NLRC5, and CIITA directly activate the downstream signaling pathways; NLRP1, NLRP3, NLRP6, NLRP7, NLRP12, NLRC4, and NAIP are known to function through inflammasome formation (Zhong *et al.*, 2013). Activated NOD1 and NOD2 lead to autophosphorylation of Rip2 kinase, which results in the

activation of MAPK and NF κ B signaling pathways. NLRs, which form inflammasome recruits ASC after the ligand interaction, activate the caspase-1 to induce the processing and secretion of IL-1B. (Kim *et al.*, 2016) On the other hand, CIITA causes the transcription of MHCII via recruitment and the interaction of the enhanceosome complex, and NLRC5 leads the transcription of MHCI (Kim *et al.*, 2016; Liu *et al.*, 2019).

The importance of NLRs and their possible roles in diverse mechanisms can be indicated by their association with many diseases. NOD1 and NOD2 are linked with chronic inflammatory conditions such as asthma, atopic eczema and dermatitis, and Crohn's disease. Some of the disorders in which NLRP1 is implicated are Alzheimer's, vitiligo, celiac disease, Addison's disease, and type 1 diabetes. NLRP7 is associated with hydatidiform mole disease and abnormal embryonic development. NLRP6 is indicated to be involved in colitis and colon cancer. NLRP3 is connected to numerous conditions, including gout, inflammatory bowel diseases, type 2 diabetes, and cryopyrin-associated periodic syndromes (CAPS). (Zhong *et al.*, 2013)

1.4. Inflammasomes

Inflammasomes are multimeric protein complexes that assemble following the detection and sensing the diverse PAMPs and DAMPS within the cell and subsequently induce the inflammatory response. Inflammasomes typically form around a sensor protein and recruit an inflammatory caspase directly or through an adaptor protein, Apoptosis-associated Speck-like protein containing CARD (ASC). The inflammasome formation is activated via various exogenous and endogenous signals deriving from pathogens, microbiome, or host. (Zheng *et al.*, 2020) Inflammasome assembly starts with the sensor/scaffold protein interaction with its ligands. Some scaffold proteins known to assemble into inflammasomes are NLRs, including NLRP3, NLRC4, NLRP6, NLRP7, and NLRP12, and non-NLR proteins like AIM2 and PYRIN (Guo *et al.*, 2015). These inflammasome-forming proteins are expressed in various cell types such as macrophages, neutrophils, and dendritic cells (Zheng *et al.*, 2020). They sense a plethora kind of stimuli. While AIM2 senses DNA, NLRC4/IPAF inflammasome is

activated by the bacterial type III secretion system, and flagellin and NLRP1 inflammasome assemble when it encounters lethal anthrax toxin from *Bacillus anthracis*. NLRP3, the most-studied inflammasome, is activated by a vast number of stimuli such as alum, uric acid, pore-forming toxins, ATP, and potassium efflux. (Vanaja *et al.*, 2015).

In canonical activation of the inflammasome, pro-caspase-1 is either recruited by the CARD domain with homotypic binding or through the ASC in the existence of a Pyrin domain after the sensor protein binds to the ligand. Caspase 1 is a cysteine protease found as an inactive zymogen in the cytosol, and following the recruitment to the inflammasome, it is activated with autophosphorylation. Active caspase-1 cleaves the pro IL-1 β to activate for its release (Strowig *et al.*, 2012). Caspase 1 is also able to cleave the IL-18 and gasdermin-D. Upon the cleavage and release of its N-terminal domain, Gasdermin-D oligomerizes to form pores in the plasma membrane to start the pyroptosis process, which is a form of cell death (Deets and Vance, 2021). In non-canonical inflammasome activation, caspase-11 is activated upon the detection of intracellular LPS, which leads to the assembly of the NLRP3 inflammasome, resulting in cell death and IL-1 α secretion in mice. In human, caspase-4 and caspase-5 activates the NLRP3 inflammasome independent of the NLRP3 activation as a pattern recognition receptor (Guo *et al.*, 2015).

Inflammasome activation is an essential innate response to infection and tissue damage to control the invasion. However, the dysregulated inflammasome activation may give rise to the development of various diseases such as cancer, autoimmune disorders, and neurodegenerative and metabolic diseases. Therefore, tight regulation in inflammasome activation and inhibition is required to limit the harm while still controlling the infection. (Zheng *et al.*, 2020)

1.5. NLRP13

NLRP13 is an NLR with an N-terminal effector domain which has Pyrin, central NOD domain, and C-terminal LRR domain. It is also known as NALP13, NOD14,

CLR19.7, and PAN13. NLRP13 gene located on located on 19q13.43 for *Homo sapiens*, consists of 12 exons and produces 118 kDa protein. Two splice variants with the sizes of 1036 and 1043 amino acids are known. It is found in humans, bovines, dogs, and chimpanzees, not in rodents.

NLRP13 is a maternal effect expression gene, its expression is high in oocytes and gradually decreases in developing embryos (Zhang *et al.*, 2008). Its expression is increased upon *Toxoplasma gondii* infection in THP-1 macrophages (Wang *et al.*, 2016). It is also known that doxorubicin-resistant U87 glioblastoma cells harness a missense mutation in NLRP13 (J. Han *et al.*, 2016). Also, a recent paper shows that the patients who died from HIV and tuberculosis co-infection had significantly lower NLRP13 expression when compared to the survived patients (Gebremicael *et al.*, 2022).

Our knowledge of NLRP13 comes from our former Master thesis students, Yetiş Gültekin, Mustafa Yalçınkaya and Açıya Yılmaz. Yetiş Gültekin showed that NLRP13 is mainly found in the cytosol and partly in the mitochondria. Co-immunoprecipitation experiments showed weak interaction of NLRP13 with ASC and Caspase-1 but not with Caspase-1. NLRP13 forms inflammasome-like structures in overexpression models. Mustafa Yalçınkaya's study demonstrated that the LPS/ATP treatment leads to increase in THP-1 macrophages indicating that ATP is the inducer of NLRP13 expression.

Also, the cytokine profiling was displayed an increase in the cytokines IL-6, IL-6Sr, IL-1 β , GM-CSF, TNF- α and RANTES (CCL5) Açıya Yılmaz's study was focused on the NLRP13 inflammasome activation. Inflammasome activation and the pro-inflammatory response were demonstrated to be increased upon LPS/ATP treatment and *P. aeruginosa* infection in NLRP13 overexpressed THP-1 macrophages. She also showed that NLRP13 is cleaved by Caspase-8 in vitro.

1.6. Caspases

Caspases are a family of cysteine proteases that are primarily known for their roles in cell death. They contain an N-terminal protease domain that has large and catalytic subunits that operates the hydrolyzation after specific aspartic acid residues in their substrates. (van Opdenbosch and Lamkanfi, 2019)

Functionally, caspases can be divided into two main groups as apoptotic and inflammatory caspases. Apoptotic caspases can be further classified into two subgroups as initiator caspases which are caspases 2, 8, 9, 10, and executioner caspases which are caspases 3, 6, and 7. (van Opdenbosch and Lamkanfi, 2019). All caspases include a C-terminal domain which operates the proteolytic cleavage of their substrates (Kesavardhana *et al.*, 2020). Initiator caspases comprise either a caspase recruitment domain (CARD) as in caspase 9 or death effector domains (DED) as in caspase 8 and 10. These domains activate and recruit multiprotein complexes. For the activation of the initiator caspase, they first dimerize with a proximity-driven mechanism. This action results in conformational changes through which the flexible regions between the small, the large and the pro-domain subunits are auto-cleaved. Initiator caspases later activate the executioner caspases which do not include an N-terminal pro-domain. (van Opdenbosch and Lamkanfi, 2019). Caspase 1, 4, 5, 11 and 12 are involved in the inflammation, they also contain the CARD domain and can auto-preotypically cleave themselves (Kesavardhana *et al.*, 2020).

Caspases have a diversity of functions other than apoptosis and inflammation. Caspase 3 has many roles including lamin B and acinus cleavage, lens fiber formation, bone and osteoblast formation, differentiation migration and plasticity of neurons, and stem-cell quiescence. Caspase 2, caspase 3, and caspase 9 participate in the lamin B and acinus cleavage, while caspase 3 and caspase 9 were known to be related to the formation of muscle fiber. Caspase 3, caspase 8, and caspase 9 seem to be associated with macrophage formation. (Shalini *et al.*, 2015)

1.7. Caspase 8

Caspase 8 is mainly known to be the initiator of extrinsic apoptosis following the activation of death receptors. Its inactive form, pro-Caspase-8, is a single-chain inactive zymogen and proteolyzes in trans after being recruited to the DISC. (Mandal *et al.*, 2020) DISC is the death inducing signaling complex which forms upon fas ligand binding to fas receptor, and recruitment of FADD, a cytosolic adaptor protein (Cullen and Martin, 2009). The inactive precursor of caspase 8 (p55/p53) consists of two N-terminal death effector domains (DEDs) and a C-terminal protease domain with large and small subunits, which are p18 and p10, respectively. For the maturation of Caspase 8, two pro-caspase-8 are dimerized and auto-processed. Initially, the linkage between p18 and p10 subunits are cleaved, and this action is followed by the cleavage of p18 and the pro-domain. Subsequently, two p18 and two p10 subunits constitute the mature caspase-8. (J. H. Han *et al.*, 2021)

Although having the primary function as the apical initiator caspase of apoptosis, caspase-8 is also involved in additional roles of mediating the crosstalk between the different cell death mechanisms and inflammatory response. It can cleave Caspase-3 and bid to lead to apoptosis or target Receptor-interacting protein kinase (RIPK)1, RIPK3, and cylindromatosis (CYLD) to inhibit necrosis. It also contributes to an inflammatory response by promoting the cleavage of IL-1 β directly and processing GSDMD that leads to pyroptosis, activation of inflammasome formation and NF- κ B pathway, and the regulation of cytokine transcriptional responses. (J. H. Han *et al.*, 2021)

Expression Caspase-8 seems to be downregulated in many cancer types such as breast cancer, colorectal cancer, hepatocellular carcinoma, prostate cancer, ovarian cancer, and neuroblastoma (Mandal *et al.*, 2020).

Caspase 8 deficiency has been shown to lead an increase in polarization towards M1 through RIPK activation (Cuda *et al.*, 2015). And, it is speculated that caspase-8 expression has a role in macrophage polarization (Kostova *et al.*, 2021).

1.8. Macrophage Polarization

Monocytes derive from the progenitors of the bone marrow, and they migrate into tissues using the bloodstream. In the case of homeostasis and inflammation, they differentiate into macrophages or dendritic cells in the tissue where they encounter diverse factors, including pro-inflammatory cytokines, microbial components, and growth factors. (Shi and Pamer, 2011)

Macrophages are a heterogeneous population of phagocytes of the innate immune system, and they play an essential role in effectively controlling and clearing infections. Macrophages can polarize into various types that can be differentiated by phenotype and function as a response to different stimuli from the microenvironment. The two principal polarization states are classically activated M1 and alternatively activated M2, their roles are mainly pro-inflammatory and anti-inflammatory, respectively (Raggi *et al.*, 2017). M1 macrophages form during infection and help the host fight against pathogens. However, excessive action of M1 may cause redundant tissue damage and homeostasis needs to be retained. Therefore, M2 macrophages emerge to repair damaged tissue also for remodeling and vasculogenesis (Shapouri-Moghaddam *et al.*, 2018).

M1 macrophages are activated upon exposure to lipopolysaccharide (LPS) or Th1 cytokines like IFN- γ , GM-CSF, and they form pro-inflammatory related cytokines such as IL-1 β , IL-6, IL-12, IL-23, and tumor necrosis factor (TNF)- α . On the other hand, polarization towards M2 macrophages happens with Th2 cytokines such as IL-4 and IL-13 and creates an anti-inflammatory response with cytokines like IL-10 and TGF- β . They display high plasticity, which allows them to switch into one another in the case of M1 or M2 macrophages detecting the activating factors of the other. (Shapouri-Moghaddam *et al.*, 2018). With the polarization, the cell surface marker of the macrophage is adjusted. CD80, CD86, and CD16/32 are particularly displayed on M1 macrophages, and M2 macrophages express arginase-1 (Arg-1), mannose receptor (CD206), IL-10, and chemokines such as CCL17 and CCL22 (Yunna *et al.*, 2020).

2. HYPOTHESIS AND PURPOSE

NLRP13 is a novel protein from the NOD-like receptor family that contains NOD, PYRIN, and LRR domains. In our lab, it has been shown that NLRP13 was found in the cytosol along with partly mitochondria. It interacts with inflammasome components ASC and Caspase-1 in the overexpression model of HEK293FT. LPS/ATP and *Pseudomonas Aeruginosa* infection are the inducers of NLRP13 expression and lead to an increased pro-inflammatory response in NLRP13 overexpressed THP1 macrophages. It was also exhibited that Caspase-8 cleaves NLRP13.

The first aim of this project was to determine the localization of cleaved forms of NLRP13. For this purpose, a construct that will express an NLRP13 protein with HA-tag at the C-terminal and FLAG-tag at the N-terminal was produced. This vector was cotransfected to HEK293FT cells with fluorescent protein-tagged organelle marker plasmids (MTS-DsRED, Rab5, Rab9, Rab11), and immunofluorescence was performed with antibodies against HA and FLAG to visualize under confocal microscopy. The localization of two terminals of NLRP13 was observed upon endogenous Caspase-8 activation by utilizing the Fas-receptor antibody binding and activating the Fas-ligand receptors on HEK293FT cells. The second object of the project was to understand whether NLRP13 has a role in macrophage polarization. Considering the M1 macrophage-like cytokine profile of NLRP13 stable THP1 macrophages and NLRP13's relationship with Caspase-8, it was hypothesized that NLRP13 might be participating in macrophage polarization. To determine NLRP13's possible function in macrophage polarization, WT, mCherry plasmid control group, and NLRP13 overexpressing THP1 cells were polarized into M1 and M2 macrophages. Following macrophage polarization assay, M1 and M2 marker levels for mRNA and cell surface proteins were compared. It was also aimed to knock down NLRP13 in THP1 cells using CRISPRi/CAS9 system to further analyze the upstream and downstream pathways of NLRP13. Overall, the localization of cleaved forms of NLRP13 and its possible role in macrophage polarization, and its knockdown were studied.

3. MATERIALS

3.1. Cell Lines

3.1.1. Human Embryonic Kidney Cell Line (HEK293FT)

The HEK293FT is a cell line originating from the kidney tissue of a female fetus. This cell line was kindly provided by Prof. Maria Soengas from the Spanish National Cancer Research Center (CNIO, Madrid, Spain) and grown in DMEM includes of 10% FBS, 100 U/ml penicillin, 100 µg/ml streptomycin and 1X MEM Non-Essential Amino acids.

3.1.2. THP1 Monocytic Cell Line

The THP1 is a human monocytic cell line derived from acute leukemia. This cell line kindly provided by Prof Ahmet Gül of Istanbul University (Istanbul, Turkey) and grown in RPMI-1640 medium consists of 10% FBS, 100 U/ml penicillin, 100 µg/ml streptomycin and 1X MEM Non-Essential Amino acids.

3.2. Chemicals, Plastics and Glassware

Chemicals were purchased from Applichem (Germany), Merck (Germany), or Sigma (USA). Plastics were acquired from Axygen (USA), TPP (Switzerland), or VWR (USA). Before usage, the sterilization of glassware, tubes and tips was ensured by autoclaving at 121°C for 20 minutes.

3.3. Buffers and Solutions

3.3.1. Cell Culture

Table 3.1. Cell culture chemicals.

Chemicals	Supplier/Recipe
Dulbecco's Modified Eagled Medium	PAN Biotech, Germany
RPMI Media 1640	Gibco Invitrogen, USA
ATP	Sigma, USA
DMSO	Applichem, Germany
Puromycine	Sigma, USA
Fetal Bovine Serum	Gibco Invitrogen, USA
Penicilin/Streptomycin	Gibco Invitrogen, USA
PMA	Sigma, USA
LPS	Sigma, USA
MEM Non-essential amino acid 100X	Gibco Invitrogen, USA
PBS 10X	80 gr NaCl 2gr KCl 2.4 gr KH_2PO_4 14.4 gr Na_2HPO_4 Add ddH ₂ O up to 1 lt (pH:7.2)
PBS-EDTA	10 mM EDTA 1X PBS, pH: 8,0

3.3.2. Molecular Cloning

Table 3.2. Enzymes used in cloning.

Buffers/Enzymes	Supplier/Recipe
SalI	NEB USA
T4 DNA Ligase	NEB, USA
T4 DNA Ligase Buffer	NEB, USA
Q5 DNA Ligase	NEB, USA
Q5 DNA Ligase Buffer)	NEB, USA
DpnI	NEB, USA

3.3.3. Transfection and Transduction.

Table 3.3. Transfection and transduction reagents.

Reagents	Supplier/Recipe
CaCl ₂	Merck, USA
HEPES	Gibco Invitrogen, USA
Polybren	Sigma, USA
2X HBS Buffer	50 mM HEPES pH 7.0 280 mM NaCl Na ₂ HPO ₄

3.3.4. Western Blotting

Table 3.4. Chemicals used in SDS-PAGE gel preparation.

Chemicals/Solutions	Supplier/Recipe
Acrylamide: Bisacrylamide	Applichem, Germany
Ammonium Persulfate	10 % APS (w/v)
4 % Stacking Gel	3,3 mL Acrylamide Solution 6,3 mL 0,5 M Tris-HCl, pH:6,8 250 μ L 10% SDS (w/v) 15 mL ddH ₂ O
10 % Stacking Gel	3,4 mL Acrylamide Solution 2,6 mL 2,6 M Tris-HCl, pH:8,8 100 μ L 10% SDS (w/v) 3,8 mL ddH ₂ O
15 % Stacking Gel	5,0 mL Acrylamide Solution 6,3 mL 2,6,5 M Tris-HCl, pH:8,8 100 μ L 10% SDS (w/v) 2,2 mL ddH ₂ O

Table 3.5. Solutions used in Western Blotting.

Solutions	Supplier/Recipe
Blocking Solution	5% non-fat milk in TBS-T
RIPA Buffer	25 mM Tris-HCl, pH:7,6 150 mM NaCl 1% NP-40 (w/v) 1% sodium deoxycholate (w/v) 0.1% SDS (w/v)
5X Laemmli Sample Buffer	1.25 M Tris-Hcl (pH:6,8) 5 mL 2-mercaptoethanol 5 mL 10% SDS 20 mL Glycerol 10 mL 0,5% bromophenol blue in ddH ₂ O 5 mL
10X Running Buffer	30,3 g Tris-base 144,1 g Glycine, 10 g SDS up to 1 L ddH ₂ O
10X TBS	24 g Tris-base, 88 g NaCl up to 1 L ddH ₂ O
1X TBST (0,1 %)	1X TBS 1 L 1 mL Tween-20
10X Tris Glycine Buffer	30 g Tris-base, 144 g Glycine up to 1 L ddH ₂ O
1X Wet Tansfer Buffer	100 mL 10X Tris Glycine Buffer 200 mL methanol up to 1 L ddH ₂ O
Stripping Buffer (mild)	7,5 g glycine 0,5 g SDS 20 mL Tween-20 up to 500 mL ddH ₂ O, pH:2,2

Table 3.6. Chemicals used in Western Blotting.

Chemicals/Solutions	Supplier/Recipe
Bovine Serum Albumin Fraction V	Roche, Germany
2-Propanol	Merck, USA
Methanol	Merck, USA
SDS	Sigma-Aldrich, USA
TEMED	Merck, USA
Tween-20	Sigma-Aldrich, USA
Pageruler Prestained Protein Ladder (26616)	Thermo Fisher Scientific, USA
PVDF Membrane	Merck, USA
WesternBright ECL HRP substrate	Advansta, USA
WesternBright Sirius HRP substrate	Advansta, USA

3.3.5. Culture of Bacteria

Table 3.7. Chemicals used in culture of bacteria.

Chemicals	Supplier/Recipe
Ampicillin	AppliChem, Germany
LB Agar	1 L LB medium 15 g Agar
LB Medium	10 g Tryptone 5 g Yeast Extract 5 g NaCl

3.4. Fine Chemicals

3.4.1. Plasmids

Table 3.8. Plasmids.

Plasmids	Provider
MTS-DsRED	AKLAB, Bogazici University
pcDNA3-Flag-NLRP13	AKIL, Bogazici University
pCFP Rab5	Batu Erman Lab., Bogazici University
pCFP Rab9	Batu Erman Lab., Bogazici University
pCFP Rab11	Batu Erman Lab., Bogazici University
pLKO5.sgRNA.EFS.GFP	GenReg, Bogazici University

3.4.2. Primers

Table 3.9. Primers used in RT-qPCR and Sanger sequencing.

Primer	Sequence (from 5' to 3')	Application
GAPDH F	GGAGCGAGATCCCTCCAAAAT	RT-qPCR
GAPDH R	GGCTGTTGTCATACTTCTCATGG	RT-qPCR
CD80 F	AGTACAAGAACCGGACCATC	RT-qPCR
CD80 R	GGCGTACACTTTCCTTCTC	RT-qPCR
CD206(MRC1) F	CTACAAGGGATCGGGTTTATGGA	RT-qPCR
CD206(MRC1) R	TTGGCATTGCCTAGTAGCGTA	RT-qPCR
NLRP13 F1	ATCCAAACCAAGAAGAACCAGAG	RT-qPCR
NLRP13 R1	TGGTCTTTAGGCCAACTGATGTT	RT-qPCR
NLRP13 F2	AACTTGAGAGCTGCCGACC	RT-qPCR
NLRP13 R2	TCTCTAGATCTTCCTGGGTTG	RT-qPCR
sg3 PCR F	TGATGGCCCTGGATCAGTAT	Sequencing
sg3 PCR R	TGCTACTCCTTCCCAGGCTA	Sequencing
sg6 PCR F	AATGTGCTTAGCGTGTGCTG	Sequencing
sg6 PCR R	GCAAACGGGATTGAAGAGA	Sequencing

3.4.3. Oligos

Table 3.10. Oligos used in cloning.

Primer	Sequence (from 5' to 3')
HA PI F	TGAAAAAGTCGACATGCAGGCTGCAGAACTCG GGTACCCATACGATGTTCCAGATTACGCTGGATA CCCATACGATGTTCCAGATTACGCT
HA PI R	ACTTGCATTAGTGA ACTATAGAATAGGGCCGCTTA AGCGTAATCTGGAACATCGTATGGGTAAGCGTAA TCTGGAACATCGTATGGGTATCC

3.4.4. Antibodies

Table 3.11. Antibodies.

Antibodies	Host/Isotype	Supplier
β Actin	Rabbit	CST, USA
Alexa Fluor 488 anti-Mouse	Donkey/IgG	Life technologies, UK
Alexa Fluor 555 anti-Rabbit	Donkey/IgG	Life technologies, UK
Anti-mouse IgG HRP	Mouse	CST, USA
Anti-rabbit IgG HRP	Rabbit	CST, USA
APC/Cyanine7 CD206 (MMR)	Mouse/IgG1	BioLegend, USA
Brilliant Violet 421 CD80	Mouse/IgG1	BioLegend, USA
Caspase-8 (1C12)	Mouse	CST, USA
FLAG (F3165)	Mouse	Sigma Aldrich, USA
HA (6E2)	Mouse	CST, USA
HA (C29F4)	Rabbit	CST, USA
NLRP13 (ab105410)	Rabbit	Abcam, UK

3.5. Kits

3.5.1. Kits

Table 3.12. Kits.

Kits	Supplier
Direct-zol RNA Miniprep Kit	Zymo Research, USA
Nucleobond Xtra Plus EF Plasmid Isolation Kit	Macherey Nagel, Germany
Nucleospin Gel and PCR Clean-up Kit	Macherey Nagel, Germany
Nucleospin Plasmid Kit	Macherey Nagel, Germany
SensiFAST cDNA Synthesis Kit	Bioline, UK

3.6. Equipments

3.6.1. Equipments

Table 3.13. Equipments I.

Autoclaves	MAC601, Eyela, Japan ASB260T, Astekk, UK
Centrifuges	Allegra X22-R, Beckman, USA Himac CT4200C, Hitachi Koki, Japan J2-MC Centrifuge, Beckman, USA J2-21 Centrifuge, Beckman, USA
Freezers	2021D, Uğur, Turkey 4250T Uğur, Turkey
Flow Cytometer	BD Accuri C6, USA Sony Sh800 FACS Cell Sorter, Japan BD FACSymphony A5, USA
Incubator	PHC Europe B.V, The Netherlands
Heat Block	Thermal Shake lite, VWR, USA
Micropipettes	Rainin Mettler Toledo, USA Axygen Axygen, USA, Axypipettes, USA
Microscopes	Zeiss, Acio Observer, Germany Zeiss, Axio Observer Z1, Germany Nikon, Eclipse TS100, Netherlands
Microwave Oven	Arçelik, Turkey
Oven	Gallenkamp 300, UK
pH Meter	Hanna Instruments, USA

Table 3.14. Equipments II.

Power supply	Power Pac Universal BIO-RAD, USA
Pipettors	VWR, USA
Real-Time Quantitative PCR System	Longgene Q2000b, China
SDS-PAGE Electrophoresis System	Mini-Protean 4Cell BIO-RAD, USA
SDS-PAGE Transfer Systems	Mini Trans-Blot Cell Trans-blot Semi-Dry BIO-RAD, USA
Shaker	Polymax USA Heildophl, Germany
Softwares	ImageJ, NIH, USA FlowJo, USA Syngene-Genetools, UK Leica LASX, USA
Spectrophotometer	Nanodrop ND-100 Thermo, USA
Tube Rotator	Globe Scientific, USA
Thermal Cyclers	BIO-RAD, USA
Vortex	GmcLab, Gilson, USA
Water Bath	GFL, Germany
Water filter	UTES, Turkey
Western Blot and Agarose Gel Visualization	Syngene GBOX, UK

4. METHODS

4.1. Cell Culture

4.1.1. Maintenance of Cells

HEK293FT cells were kept in DMEM containing 10% FBS, 1% MEMNEA, and 1% Penicillin-Streptomycin. The cells were kept at 37 °C incubated with 5% CO₂.

To passage HEK293FT cells, the medium was aspirated. The cells were washed with PBS. Trypsin was added on cells and they were incubated at 37 °C for 5 minutes. The trypsin was inactivated with an equal volume of full media. The cells were collected and centrifuged at 2000 rpm for 2 minutes. The supernatant was discarded, and the cell was seeded by resolving in full media.

THP-1 cells were kept in RPMI containing 10% FBS, 1% MEMNEA, and 1% Penicillin-Streptomycin. The cells were kept at 37 °C incubated with 5% CO₂.

To passage THP1 cells, 80% of the medium was discarded and replaced with fresh medium. Or, the cells were collected and centrifuged at 1000 rpm for 5 minutes and resolved with fresh medium. These two methods were used interchangeably.

Both cell lines were approximately passaged every two days at a 1/5 ratio.

In order to freeze the cells, the pellet of the cells was resolved with 1 ml of 10%DMSO, 40% complete medium, and 50% FBS with minimal pipetting. And, they were transferred to cryotubes and kept in -80 or -150°C.

To thaw the cells, the cells were taken from the cryotubes by diluting with 4 ml of full medium. They were centrifuged and the pellet were resolved in 20% FBS containing full medium.

4.1.2. Calcium Phosphate Transfection of HEK293FT

3 million cells were seeded on 10 cm plates the day before transfection. Before the transfection final concentration of 25 μ M chloroquine was added to the medium. The transfection mix was prepared by firstly adding the plasmids, then adding 2M Calcium phosphate drop by drop. HBS was added and bubbles were produced. After 10 minutes of incubation at RT, the transfection mix was added to the plates. 6-8 hours later, the medium was changed to complete medium. 48 hours later transfection efficiency was checked.

4.1.3. Transduction of THP1 Cells

1 million of Cas9 stable THP-1 cells were seeded to 6 well plates with 1 ml full RPMI media. 2 μ g/ml polybrene was added to a filtered, fresh virus-containing medium and waited for 5 minutes. 1 ml virus was added to each well. The plate was centrifuged at 2900 rpm for 90 minutes. The medium was changed to a fresh medium after 24 hours. The GFP expression was controlled with flow cytometry 48 and 72 hours after transduction.

After the number of cells was increased, 10 million cells were taken to 10 ml of 2%FBS containing PBS and they were sorted according to their GFP expression via FACS. After sorting, they were kept at 2% Penicillin streptomycin containing full medium for 2 weeks. Then, they were sorted according to their Cas9 expression via 1 μ g/ml puromycin for 2 weeks.

4.2. Gene Expression Analysis

4.2.1. RNA Isolation

The samples were isolated with Zymo Quick RNA Miniprep Kit (AppliChem, Germany). The samples were collected with TRI reagent after PBS wash. The same amount of 100% ethanol was added on the samples and they were taken to the columns.

They were washed with Wash Buffer. DNA was digested with the mixture of DNAase buffer and DNase. After the washing steps, RNA was eluted and the amount of RNA was measured using Nanodrop 2000 (Thermo Scientific, USA).

4.2.2. cDNA Synthesis

Bioline SensiFAST™ cDNA Synthesis Kit (Bioline, UK) was used to synthesize cDNA. 1000 ng RNA was mixed with 1 µL Reverse Transcriptase and 4 µL of 5x TransAmp Buffer, and the reaction was completed to 20 ul. The samples were run at 46 °C for 20 minutes for reverse transcription and the enzyme was inactivated at 95 °C for 1 minute. Before use, the cDNA samples were completed to 100 ul.

4.2.3. RT-qPCR

For RT-qPCR, SensiFAST SYBR No-ROX Kit (Bioline, UK) was used. The reaction was prepared as in Table 4.1 and PCR was run as in Table 4.2.

Table 4.1. RT-qPCR components.

Component	Volume (μL)
SensiFast SYBR Mastermix (Bioline)	5
Forward primer (10 μM)	0,25
Reverse primer (10 μM)	0,25
cDNA (diluted 1:5)	2
dH ₂ O	2,5
Total	10

Table 4.2. qPCR conditions.

Temperature ($^{\circ}\text{C}$)	Time	Cycle
95	5 min	1
95	10 sec	35
61,5	10 sec	
72	10 sec	

4.3. Western Blotting

The samples were collected with RIPA solution and incubated at -20°C for at least an hour. 1X Laemli as the final concentration was added. The samples were incubated at 95°C for 10 minutes. SDS was prepared as 10% or 15% resolving and 4% stacking gel with glasses that has a 1,5 mm gap. After the gel was polymerized, the samples were loaded into the gel and the tank was filled with 1X running buffer. The SDS-PAGE was run at 80V at the beginning, and it was adjusted to 120V when the samples passed the stacking gel. Then, the gel was transferred to a PVDF membrane with 0,45 or 0,2 mm pore sized via the wet transfer method or the semi-dry transfer method. For wet transfer, the gel and PVDF membrane, which is activated with methanol and washed with ddH₂O, were sandwiched first between Whatmann papers, that were soaked in transfer buffer, and then between sponges. The sandwich was

placed on a tank with an ice block and ice cold 1X wet transfer buffer. The transfer was conducted at 100V for 3 hours. For the semi-dry method, the activated PVDF membrane and the gel were placed between the wet Whatmann papers and the excess waster was discarded. 30 minutes, 1 mini gel protocol was used for transfer. When the transfer is completed, the PVDF membrane was blocked with TBST containing 5% non-fat milk powder on a shaker for 1 hour at room temperature. After the blocking, the membrane was washed with TBST 3 times, 5 minutes each and the membrane was incubated with 1:1000-1:2000 antibody dissolved in 5% BSA containing TBST for 12-16 hours at +4 °C room in a 50 mL falcon on a rotator. The membrane was washed with TBST three times, 5 minutes each, and it was incubated with HRP-linked secondary antibody (1:5000-1:10000) dissolved in blocking solution. The membrane was washed 3 times and soaked in WesternBright Sirius HRP substrate mixture. The image of the membrane was taken using the Syngene-Genetools. Densitometry analysis of western blot results was completed with Fiji Image J.

4.4. Macrophage Polarization Assay

1 million THP-1 for each well of 6 well plates or 4 million cells for 10 cm^2 plate was seeded with 20 ng/ml PMA in 3% FBS, 1% Pen-Strep and 1% MEMNEAA containing medium. The media was discarded after 24 hours, the cells were washed with 1X PBS a new media containing 10% FBS, 1% Pen-Strep and 1% MEMNEAA was added to the cells. The cells were left to rest for 48 hours. For M1 polarization, the cells were treated with 20 ng/ml IFN-gamma and 10 pg/ml LPS for 24 hours. For M2 polarization, the cells were treated with 20 ng/ml IL-4 and 20 ng/ml IL-10 for 48 hours.

4.5. Flow Cytometry

The medium of the cells was withdrawn and PBS-EDTA was added to the cells. The cells were kept on ice for 30 minutes and collected with gentle scraping. 250.000 cells were used for each staining. They were washed with 1X PBS twice. 10 μ g Fc blocker was added and the samples were incubated at room temperature for 10 minutes. The samples were centrifuged at 300g for 5 min. After the supernatant was discarded,

a 1 μ L antibody was added to the samples. The cells were incubated with antibodies on ice for 30 minutes. They were washed with 1 ml 1X PBS and centrifuged at 300g for 5 min. The supernatants were discarded. The pellet was dissolved in 250 μ L PBS and read at either BD FACSymphony or Acuri C6.

4.6. Cleavage of NLRP13

4.6.1. Competent Cell Preparation

A single colony of *E. coli* TOP10 were incubated in 10 mL of LB and incubated on a shaker at 37 °C for overnight (12-16 hours). The next day, 1:50 of culture was taken to a 250 ml erlenmeyer flask containing 50 mL of LB. The culture was grown until the OD600 reached a value between 0.4-0.5. At this point, the culture was taken to ice and centrifuged for 10 minutes at 4500 rpm, 4 °C. The pellet was resuspended in 10 ml ice-cold CaCl₂ solution and centrifuged for 10 minutes at 4500 rpm, 4 °C. The supernatant was discarded and each pellet was resuspended with 10 ml of a solution containing ice-cold CaCl₂ solution. After being left on ice for 30 minutes, they were centrifuged again at 1100 g for 5 minutes. The supernatant was discarded and each pellet was resuspended with 2 ml ice-cold CaCl₂ solution. All resuspended cells were collected, aliquoted in 200 μ L and frozen in liquid nitrogen immediately. The aliquots were stored at -80 °C.

4.6.2. Transformation

E. coli TOP10 was thawed on ice for 10 minutes. Plasmid or ligation product was added onto cells with minimal pipetting. The cells were incubated on ice for 20 minutes, heat-shocked at 42°C for 60 seconds, and immediately taken to ice and were kept on ice for 5 minutes. The cells were incubated at 37 °C for 1 hour after the addition of 1 ml luria broth. Then, the cells were centrifuged at 4500 rpm for 5 minutes and 1000 μ L of supernatant was discarded. The cells were resuspended with the remaining of supernatant and spread onto LB agar plates containing ampicillin. The plates were incubated at 37 °C 12-16 hours and single colonies were picked for screening.

4.6.3. Plasmid Isolation

Single colonies were picked and inoculated to 10 ml LB broth with ampicillin in 50 ml tubes. They were incubated at 37°C for 12-16 hours on a shaker. After incubation, the plasmid DNA was isolated with an MN kit. according to the manufacturer's instructions.

4.6.4. Restriction Enzyme Digestion

Restriction enzymes were used according to NEB's instructions.

4.6.5. Polymerase Chain Reaction

In order to add HA tag to the C terminal of NLRP13 in pcDNA3 containing the NLRP13 gene with a FLAG tag at the N terminal, two consecutive PCR was performed. Firstly, the primer product was prepared by a polymerase chain reaction in 50 μ L reaction containing 1 μ L of 10 mM dNTP, 1 μ L of 10 μ M Forward primer, 1 μ L of 10 μ M Reverse primer, 0,5 μ L of Q5 enzyme and 10 μ L of 5X Q5 Buffer as in Table 4.3 and the reaction was run as in Table 4.4.

Table 4.3. First PCR components.

Component	Volume (μL)
Forward primer (10 μ M)	1
Forward primer (10 μ M)	1
dNTP (10 mM)	1
Q5 enzyme	0,5
5X Q5 buffer	1
dH ₂ O	up to 50
Total	50

Table 4.4. First PCR conditions.

Temperature (°C)	Time	Cycle
98	3 min	1
95	3 sec	25
60	30 sec	
72	10 sec	
72	3 min	1

This PCR product was run on 0.7% agarose gel. After the confirmation, the desired band was cut under UV light and cleaned with an MN Gel Clean UP kit. The resulting PCR product was used as a double-stranded primer for the second PCR. It was designed to have homologous arms to the desired integration site. Second PCR was carried out as in Table 4.5 and Table 4.6

Table 4.5. Second PCR components.

Component	Volume/Amount
First PCR product	250 ng
Template plasmid	50 ng
dNTP(10 mM)	1 μ L
Q5	1 μ L
Q5 Buffer	10 μ L
GC Enhancer	5 μ L
dH ₂ O	up to 50 μ L
Total	50 μL

Table 4.6. Second PCR conditions.

Temperature (°C)	Time	Cycle
98	3 min	1
95	60 sec	25
60	30 sec	
72	4,5 min	
72	5 min	1

4.6.6. Agarose Gel Electrophoresis

Confirmation of the PCR products and digestion products was done with agarose gel electrophoresis. The concentration of 0.7% agarose gel was prepared with dissolving agarose in 1X TAE using the microwave oven for 2 minutes. After slightly cooled, EtBr was added for visualization of the bands under the UV light and the gel was left to polymerize. DNA samples were mixed with 6X loading dye to the final concentration of 1X and loaded into the wells. Generuler mix DNA Ladder was also loaded into a gel. The gel was run at 100V for 30 min - 1 hour according to the size of DNA and visualized with Syngene-Genetools.

4.7. Statistical Analysis

The statistical analyses were performed with GraphPad Prism 8 (San Diego, USA). For the analysis of colocalization percentage, unpaired t test was applied; for qPCR analysis multiple compared was applied following 2way ANOVA. The bars indicate the mean with SD and significance was presented as * $p \leq 0.05$, ** $p < 0.01$, *** $p < 0.001$, **** $p < 0.0001$.

5. RESULTS

5.1. Cleavage of NLRP13

5.1.1. Cloning of HA-tag to NLRP13-FLAG

It was aimed to add an HA tag to the C-terminal of NLRP13 in the pcDNA3 plasmid containing the NLRP13 gene with a FLAG sequence at the 5' end to follow the localization of NLRP13 after probable cleavage by Caspase 8.

For this purpose, FLAG-NLRP13-pCDNA3 plasmid was used. Forward and reverse primers that contain HA sequence along with the homology to the 5' end of NLRP13 gene were designed, sequences of which can be seen in Table 3.9. Forward primer consists of a complementary region to the downstream of NLRP13 gene, and reverse primer contains a complementary region to the complementary region to 5'.

Using these primers, HA sequences with proper flanking were amplified using PCR. The PCR was expected to generate a 154 base pair product with 84 base pairs of HA sequences and 79 base pairs of flanking sequences. The size of the PCR product was confirmed via 0.7% agarose gel electrophoresis which was run at 100V and visualized with the help of ethidium bromide. (Figure 5.1).

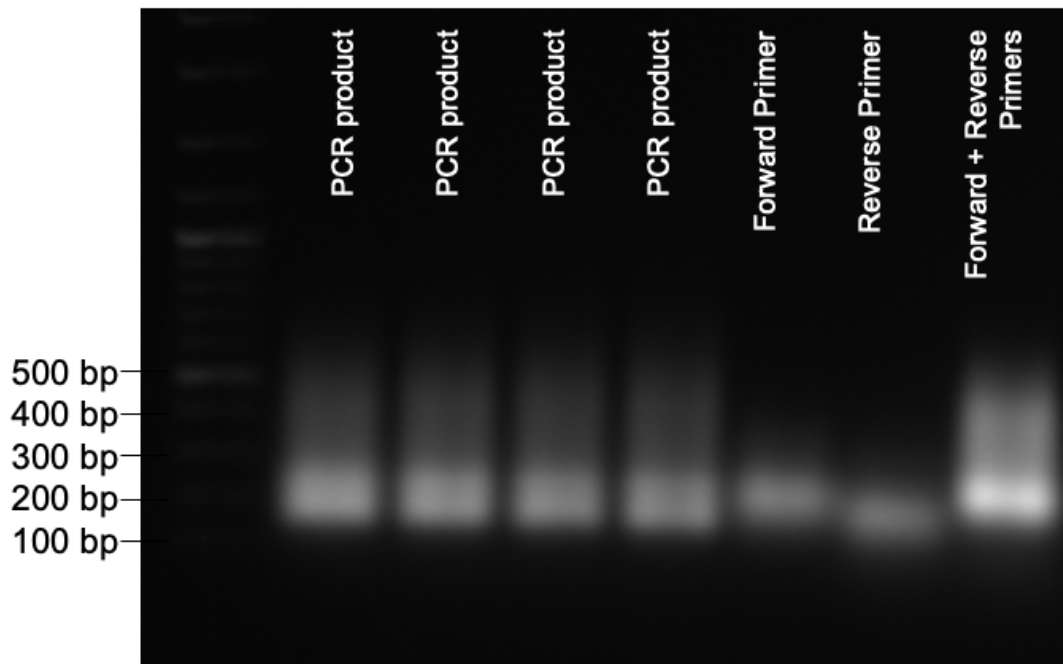


Figure 5.1. Agarose gel confirmation of the PCR product.

After visualization, desired DNA fragments were sliced from the gel and purified to separate from the gel. The acquired PCR product was used as the primer in the second PCR. In the second PCR, NLRP13 gene containing FLAG sequence pcDNA3 was used as the template plasmid. The second PCR product was digested with DpnI to eliminate the methylated DNA and to only possess the newly produced plasmid. After the DpnI digestion, the resulting product was transformed into TOP10 *E. coli* on LB agar plates supplemented with ampicillin; the next day 6 colonies were picked and their plasmids were purified. These 6 colonies were subjected to analytical digestion with the enzymes of SalI and NotI. The digestion products were loaded into 1% agarose gel and run at 100V for 30 minutes. After seeing a similar pattern with the template plasmid for DNA fragments and deciding there is no SNP or frameshift, the samples were sent sequencing to be read with DNA sequencing using BGH-reverse primer (Figure 5.2). Colony 5 and 6 have been verified to have 2 HA tags by sequencing.

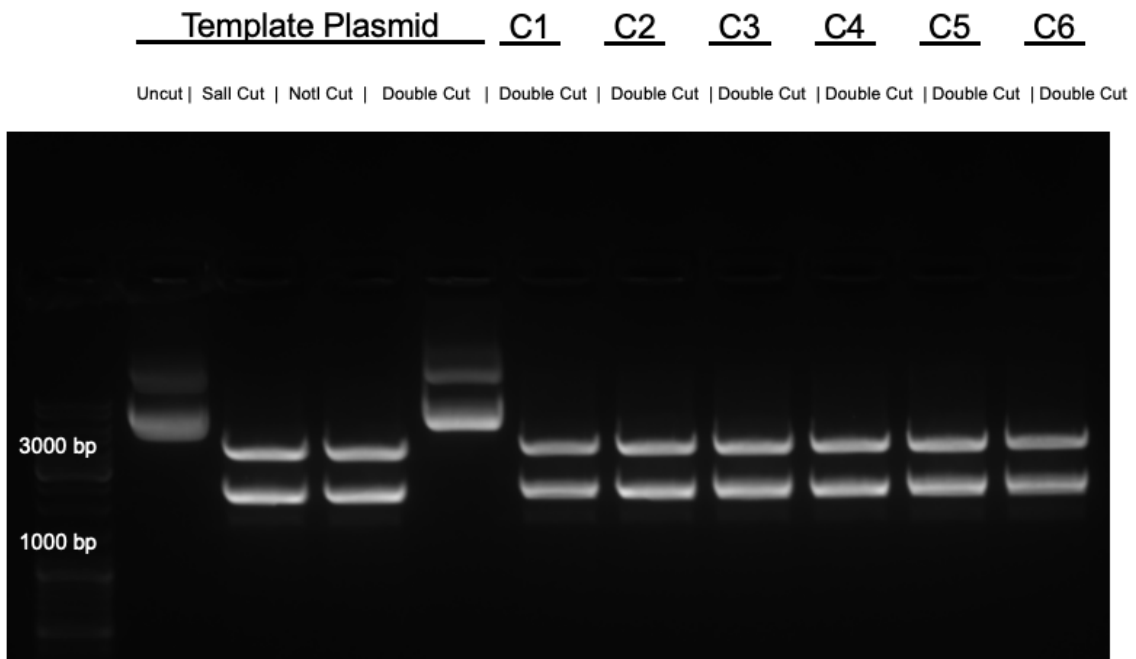


Figure 5.2. Verification of recombinant FLAG-NLRP13-HA plasmid via double digestion with Sall and NotI.

The plasmids of picked 6 colonies were also transfected to HEK293FT cells and the protein expression of HA and FLAG tags were checked. 1 μ g of plasmid for each colony was transfected into HEK293FT via the calcium phosphate method. The cells were collected after 48 hours, lysed, and run with 12% acrylamide gel initially at 80V and later at 120V with polyacrylamide gel electrophoresis. FLAG-NLRP13-HA was expected to be seen at approximately at 118 kDa. The expression of both HA and FLAG were verified by anti-FLAG and anti-HA antibodies, and anti- β -Actin was used as a loading control (Figure 5.3). It was further confirmed that C5 and C6 were appropriate to use in the following experiments.

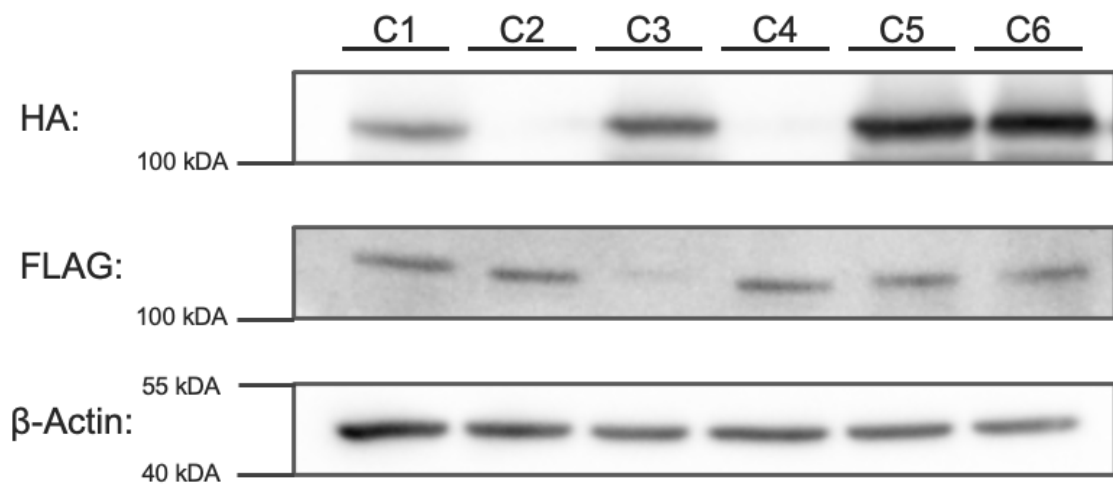


Figure 5.3. Confirmation of HA and FLAG protein expression via SDS-PAGE Western Blotting following the HEK293FT transfection of the plasmids obtained from the picked colonies.

5.1.2. Activation of Caspase-8

To cleave the transfected FLAG-NLRP13-HA, endogenous Caspase-8 was planned to be used. To be sure that the Caspase-8 is cleaved active CD95 antibody, which is a Fas-receptor antibody which acts like a Fas-ligand, was used. In its manual, 2-20 μL per test for 2-24 hours was recommended. So, different concentrations of CD95 antibody treatment were tried to observe the intermediate and the active subunits of Caspase-8, which are p43/41 and p18 (Figure 5.4). It was observed that even the smallest amounts and shortest durations lead to an increase in Caspase-8 activation (Figure 5.4). It was also seen that a little amount of active subunits of Caspase-8 could be found in the cells without any treatment (Figure 5.4).

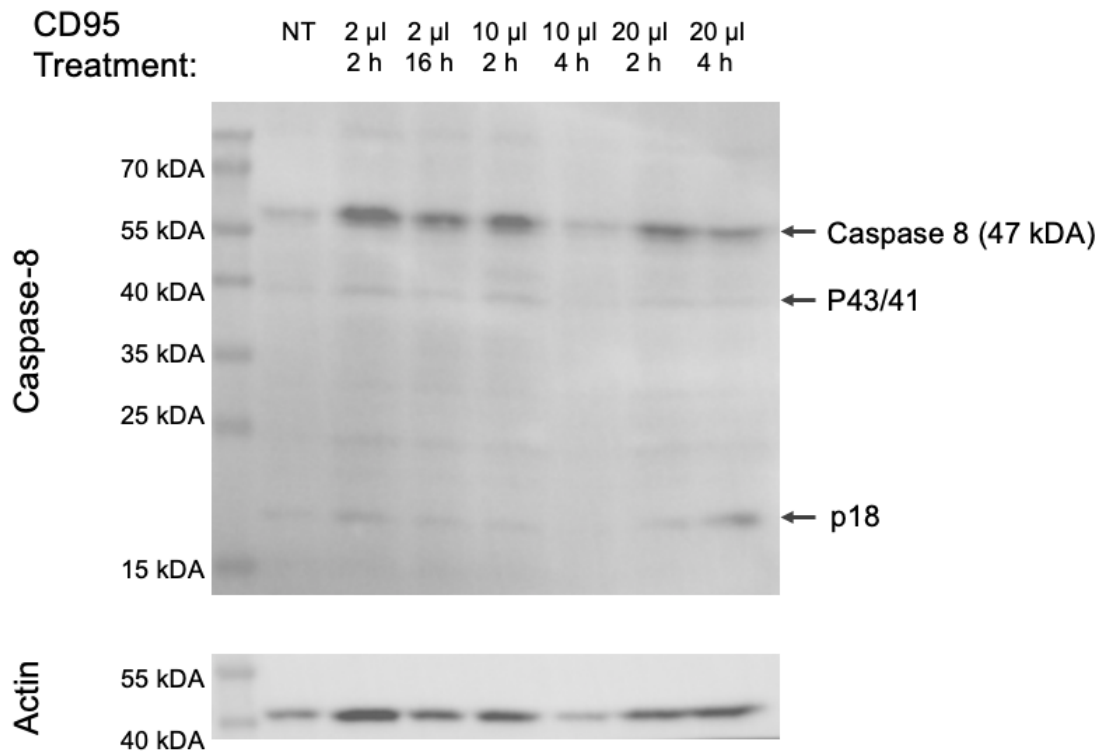


Figure 5.4. Caspase-8 activity upon CD95 treatment trial via SDS-PAGE Western Blotting.

HEK293FT cells were transfected with the FLAG-NLRP13-HA C5 and another trial of CD95 antibody treatment was performed to observe the NLRP13 cleavage. Full length of NLRP13 and cleaved forms were controlled via Western Blotting with anti-FLAG and anti-HA antibodies. Other than the non-cleaved bands of 120 kDa, an increase in the cleaved forms of NLRP13 was detected with CD95 treatment (Figure 5.5). The cleaved forms was observed as approximately 55 kDa with HA antibody, as approximately 70 kDa for FLAG antibody (Figure 5.5). The cleaved forms were also seen without any treatment, probably because of the endogenously active Caspase-8 which could be seen in Figure 5.4. 2 μ L per well for 4 hours was found to be proper for the following experiments (Figure 5.5).

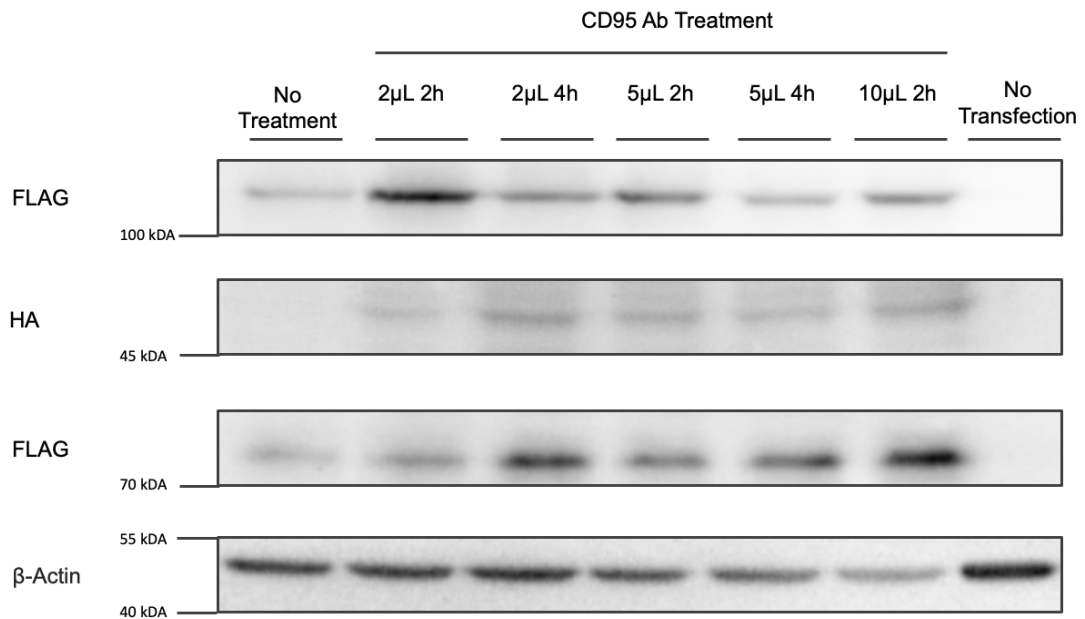


Figure 5.5. NLRP13 cleavage upon CD95 treatment trial. HEK293FT cells were transfected with FLAG-NLRP13-HA plasmid and treated with 2-20 μ L CD95 for 2-20h.

5.1.3. Immunofluorescence of NLRP13 Cleavage

To visualize the localization of cleaved forms of NLRP13, 70,000 HEK293FT cells were seeded on coverslips placed on 24 well plates. 16 hours following the seeding of cells, the cells were transfected with 250 ng FLAG-NLRP13-HA and 250 ng organelle marker plasmid, either one of MTS-DsRED, Rab5, Rab9, Rab11. 24 hours later, one group of cells was treated with CD95 antibody for 4 hours, then the cells were washed with PBS, fixed with 4% PFA and incubated with FLAG and HA antibodies after blocking with BSA/saponin. For MTS-DsRED group, Alexa 647 anti-mouse secondary was used for FLAG and Alexa-488 anti-rabbit for HA along with DAPI. For CFP-tagged Rab5, Rab9, Rab11, Alexa 555 anti-rabbit and Alexa 647 anti-mouse were used to avoid the signal leakage and DAPI could not be used due to the CFP-tag signal interference.

No colocalization between the signals of Rab5, Rab9, Rab11 and the signals of HA, FLAG was observed for the non-treated and CD95 antibody treated (+CD95) samples (Figure 5.6, Figure 5.7, Figure 5.8). It was concluded that NLRP13 does not join in endosomal intracellular trafficking.

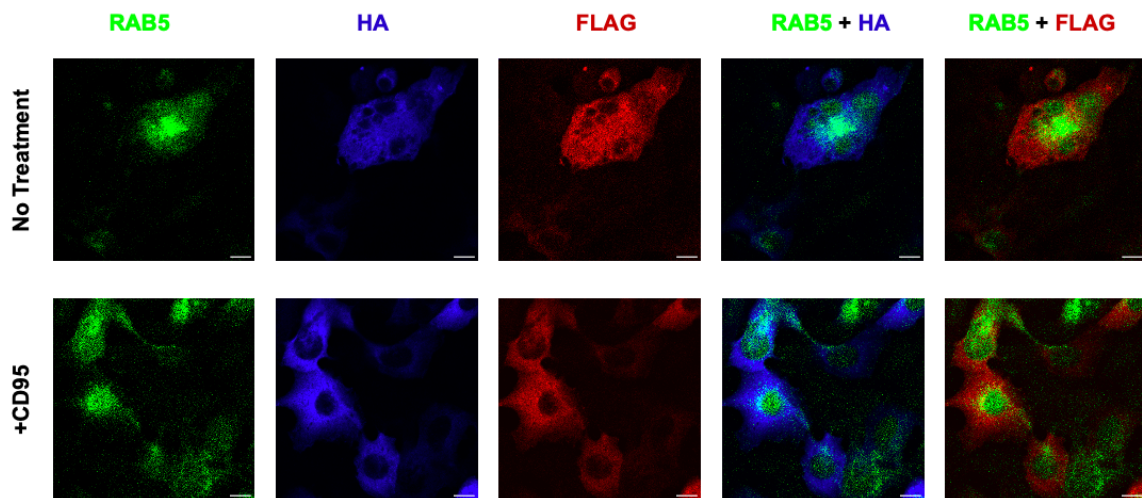


Figure 5.6. Colocalization of Rab5 with HA-tag and FLAG-tag of NLRP13. HEK293FT cells were cotransfected with FLAG-NLRP13-HA and pCFP-Rab5, then visualized with confocal microscopy after immunofluorescence using antibodies against HA and FLAG. Scale bars are 10 μ m.

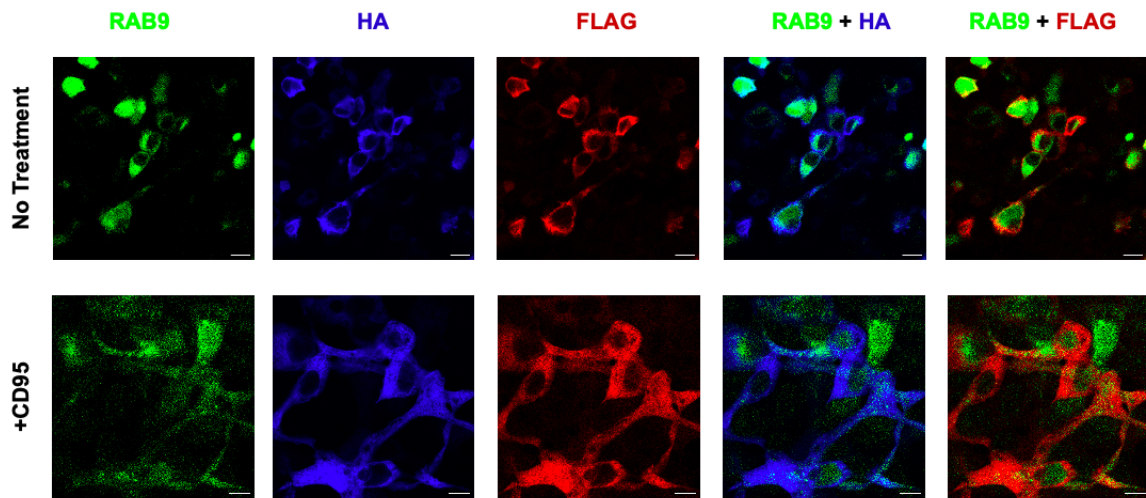


Figure 5.7. Colocalization of Rab9 with HA-tag and FLAG-tag of NLRP13. HEK293FT cells were cotransfected with FLAG-NLRP13-HA and pCFP-Rab9, then visualized with confocal microscopy after immunofluorescence using antibodies against HA and FLAG. Scale bars are 10 μm .

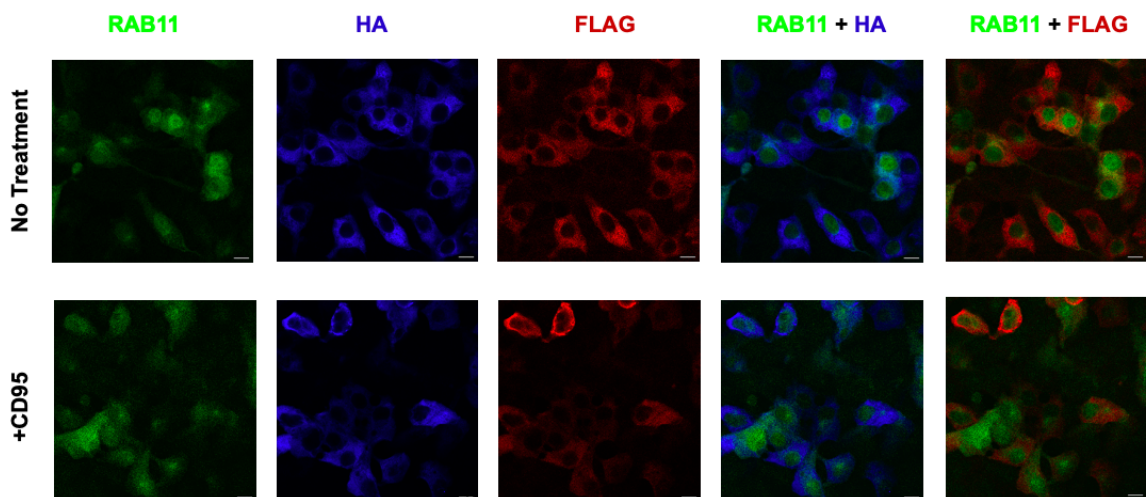


Figure 5.8. Colocalization of Rab11 with HA-tag and FLAG-tag of NLRP13. HEK293FT cells were cotransfected with FLAG-NLRP13-HA and pCFP-Rab11, then visualized with confocal microscopy after immunofluorescence using antibodies against HA and FLAG. Scale bars are 10 μm .

HA-tagged, C terminal of NLRP13 was seen to increase in the partial colocalization signal with mitochondrial MTS-DsRED upon treatment with CD95 antibody (Figure 5.9).

The colocalization was quantified using Image J. To obtain the percentage of colocalization, the green color was picked for the NLRP13 tag and red for MTS-DsRED. The area of the yellow area to the total green area was measured using the color threshold feature of Image J and the percentage was calculated using these areas. 30 cells were counted for each group. The statistical analysis was performed using Prism-Graphpad using an unpaired t-test. The increase in the colocalization percentage of NLRP13 tags with MTS-dsRED signal upon CD95 antibody treatment was found to be significant (Figure 5.10).

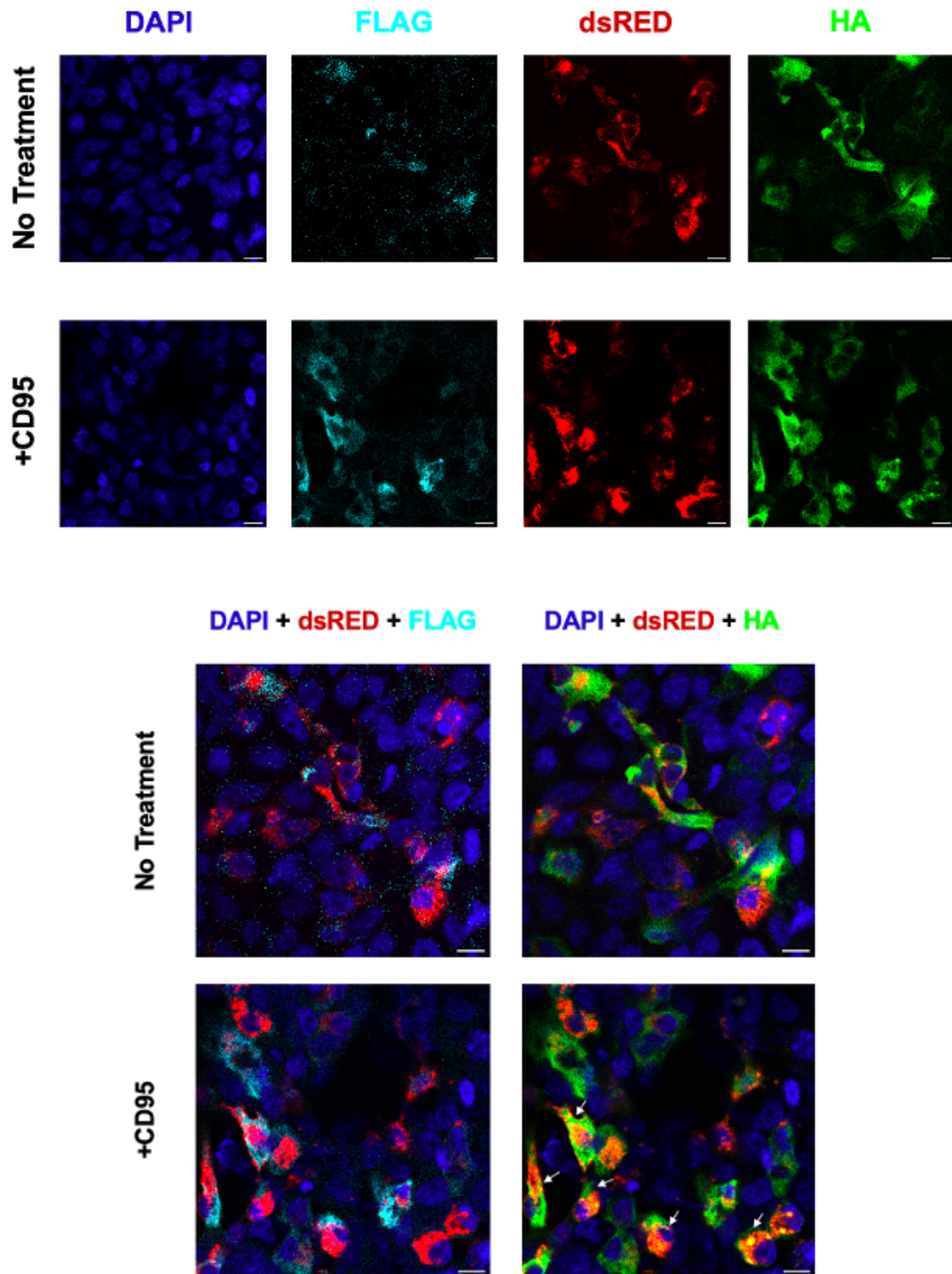


Figure 5.9. Colocalization of MTS-DsRED with HA-tag and FLAG-tag of NLRP13.

HEK293FT cells were cotransfected with FLAG-NLRP13-HA and MTS-DsRED, then visualized with confocal microscopy after immunofluorescence using antibodies against HA and FLAG. Scale bars are 10 μm.

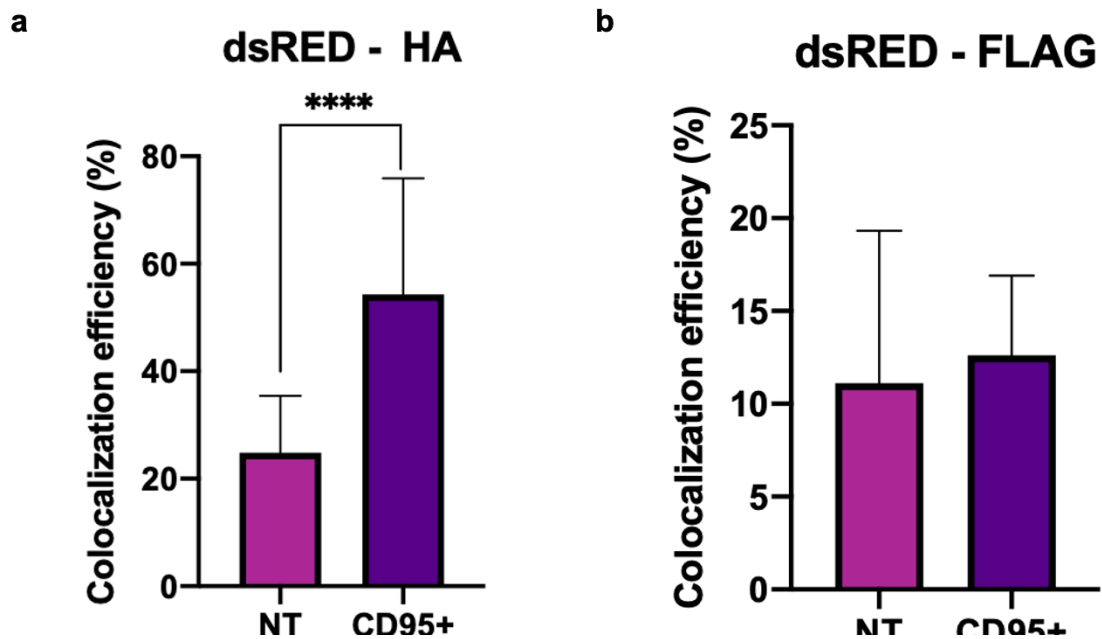


Figure 5.10. Quantification of colocalization of MTS-DsRED with HA-tag and FLAG-tag of NLRP13 via Image J. (**** $p < 0.0001$).

5.2. Macrophage Polarization

5.2.1. Optimization of Macrophage Polarization Assay

Since it was hypothesized that the NLRP13 cleavage might be involved in macrophage polarization, it was aimed to investigate the cleavage by Caspase-8 in M0, M1, M2 macrophage populations. For this, a macrophage polarization assay was designed initially. After the trial of different conditions, 20ng/ml IFN γ and 10 pg/ml for 24 hours to polarize into M1 macrophages; 20ng/ml IL4 and IL10 for 48 hours to polarize the macrophages towards M2 was found to be convenient (Figure 5.11). THP-1 monocytes were firstly differentiated into macrophages with 20 ng/ml PMA in 3% FBS containing medium. The next day, the medium was changed to a complete RPMI medium and the cells were left to rest to avoid the possible side effects of PMA. After 48 hours, the cells were polarized to M1 or M2.

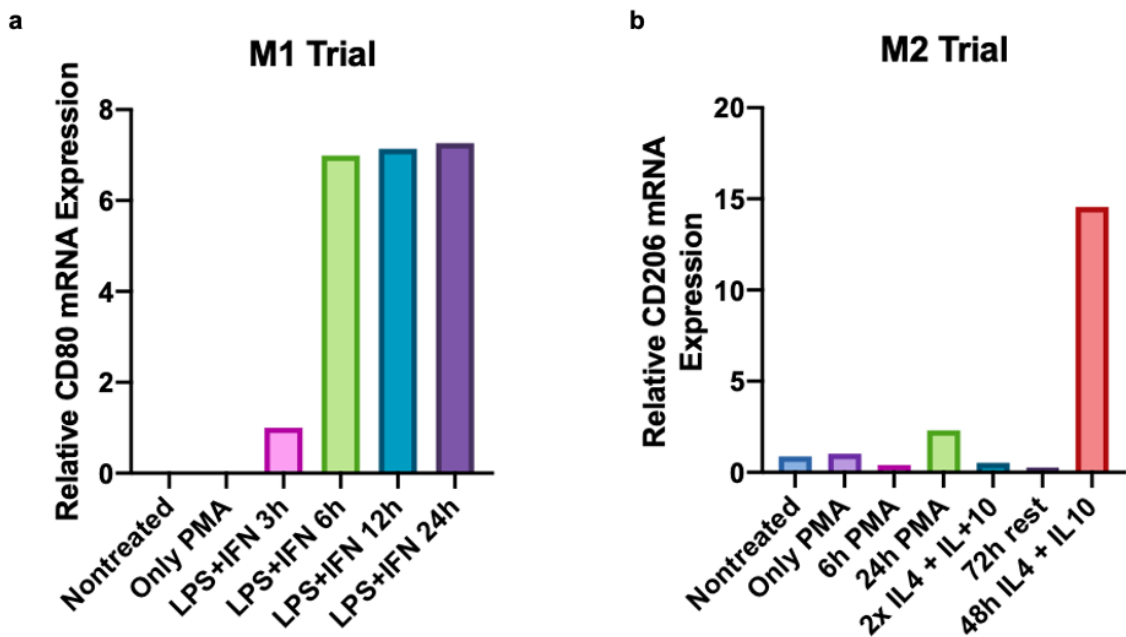


Figure 5.11. Optimization of macrophage polarization assay using RT-qPCR. (a) Relative mRNA expression of CD80. (b) Relative mRNA expression of CD206.

5.2.2. Visualization of Macrophage Polarization Assay

To see if there is a difference in the polarization towards M1 or M2, THP-1 WT, THP-1 mCherry and THP-1 NLRP13 cells were used. THP-1 mCherry cells were used as the control group of stably NLRP13 expressing THP-1 cells. Macrophage polarization assay was conducted for each group. After PMA introduction, the cells were seen to attached to the plate surface and change in morphology (Figure 5.12). Even though there is a great variety among each group, no dramatic change was observed either between different macrophage subsets or different cell groups (Figure 5.13).

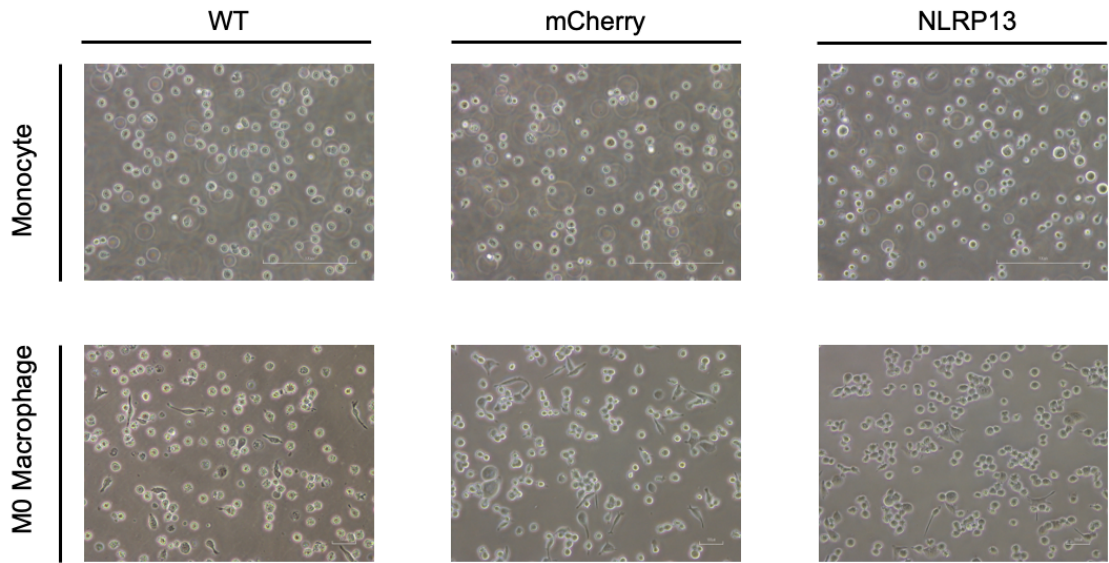


Figure 5.12. WT, mCherry and NLRP13 overexpressed THP1 nontreated monocytes and macrophages after 24 hours PMA treatment. Scale bars are 100 μm .

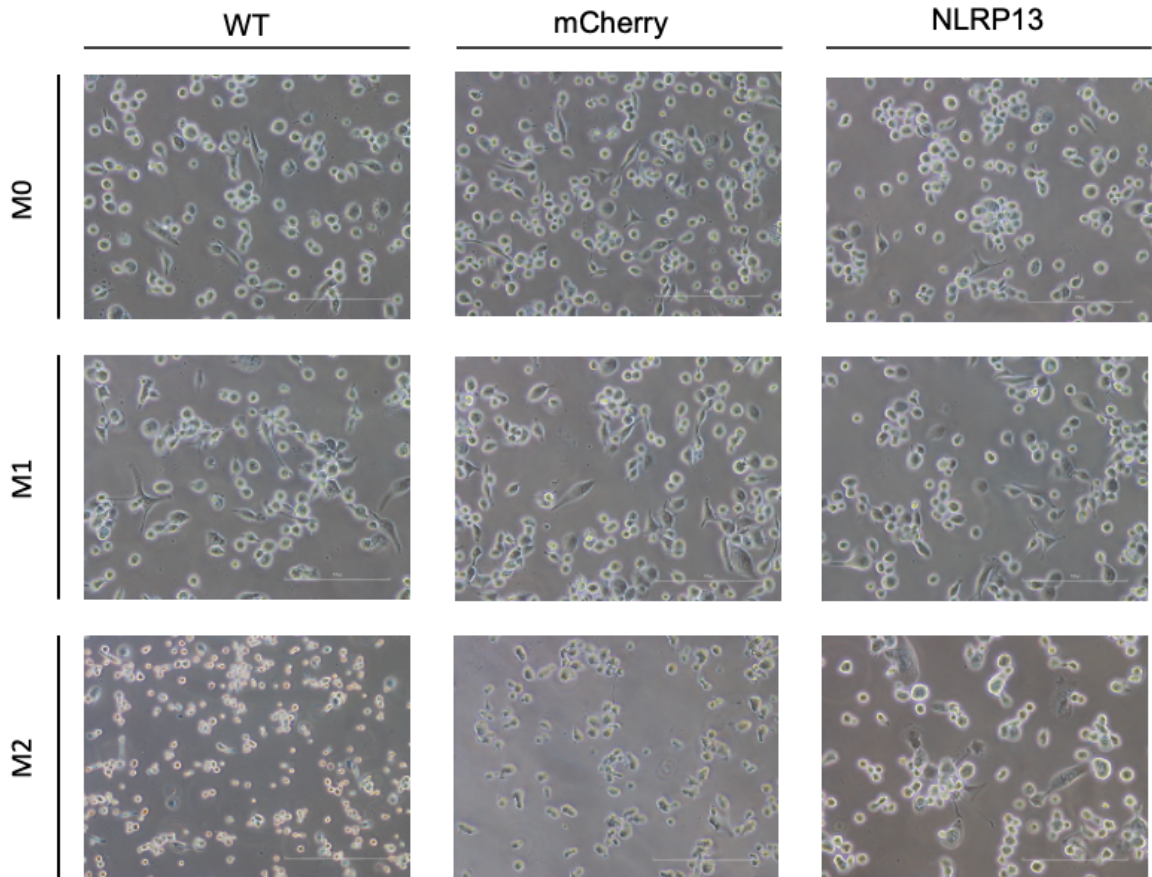


Figure 5.13. WT, mCherry and NLRP13 overexpressed THP1 M0, M1 and M1 macrophages. Scale bars are 100 μm .

5.2.3. NLRP13 Expression of Different Macrophage Subsets

NLRP13 mRNA and protein expression levels were checked upon macrophage polarization assay. No difference in mRNA expression was observed (Figure 5.14a). The expected band for NLRP13 is around 118 kDa in Western Blotting. The different subsets of macrophages were observed to express similar levels of NLRP13 (Figure 5.14b). Also, another band around 130 kDa was observed in monocytes but not in macrophages (Figure 5.14b).

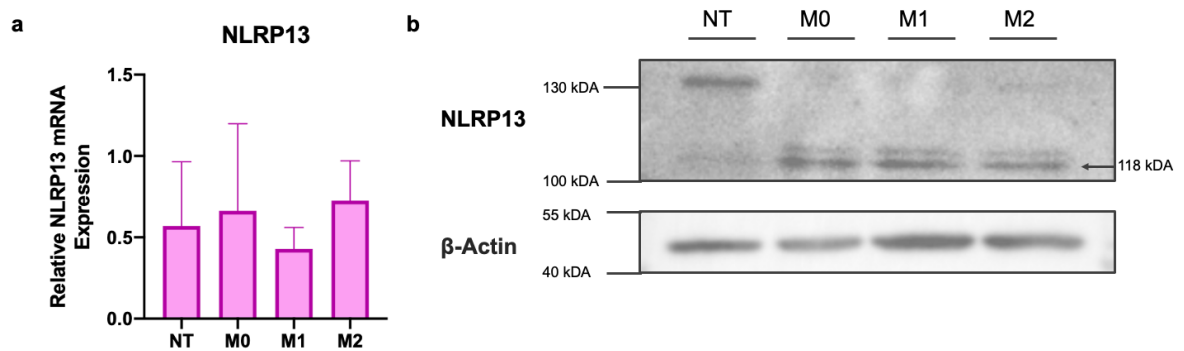


Figure 5.14. The expression of NLRP13 in monocytes, M0, M1 and M2 macrophages.

(a) The relative mRNA expression of NLRP13. (b) The protein expression of NLRP13.

5.2.4. mRNA Expression of Macrophage Polarization Assay

For the cDNA analysis, the cells were collected, and their RNA was extracted. Then, cDNA was synthesized from these RNA samples using reverse transcriptase. cDNA was amplified using primers for CD80 and CD206. The resulting signal detected by amplification was normalized to actin levels of each sample. Three biological sets were used for statistical analysis of the marker expression. Statistical analysis was performed using one-way ANOVA via GraphPad-Prism. CD80 mRNA levels of stably NLRP13 expressing THP1 macrophages were higher compared to WT and mCherry macrophages; there was no significant difference for CD206 levels (Figure 5.15).

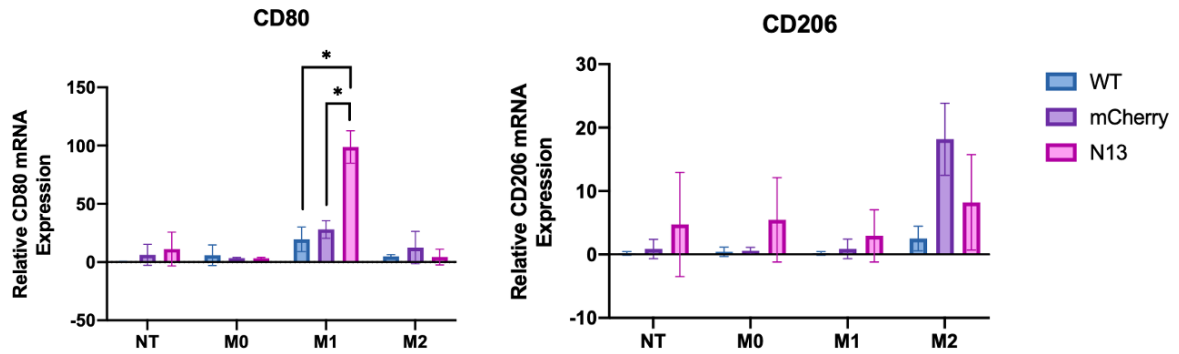


Figure 5.15. The mRNA expression of M1 marker, CD80, and M2 marker, CD206, in monocytes, M0, M1 and M2 macrophages of WT, mCherry and NLRP13 THP1. (* $p \leq 0.05$).

5.2.5. Cell Surface Marker Expression of Macrophage Polarization Assay

For flow cytometry analysis, the cells were collected with PBS-EDTA after the polarization assay. 250,000 cells were used for each staining. They were Fc-blocked and incubated with CD80 and CD206 antibodies after washing. The cells were rewashed and were read with BD FACSymphony. Similar cell populations were determined for all groups with both markers of CD80 and CD206 in all cell groups which indicated no difference in the expression of cell surface markers (Figure 5.16, Figure 5.17).

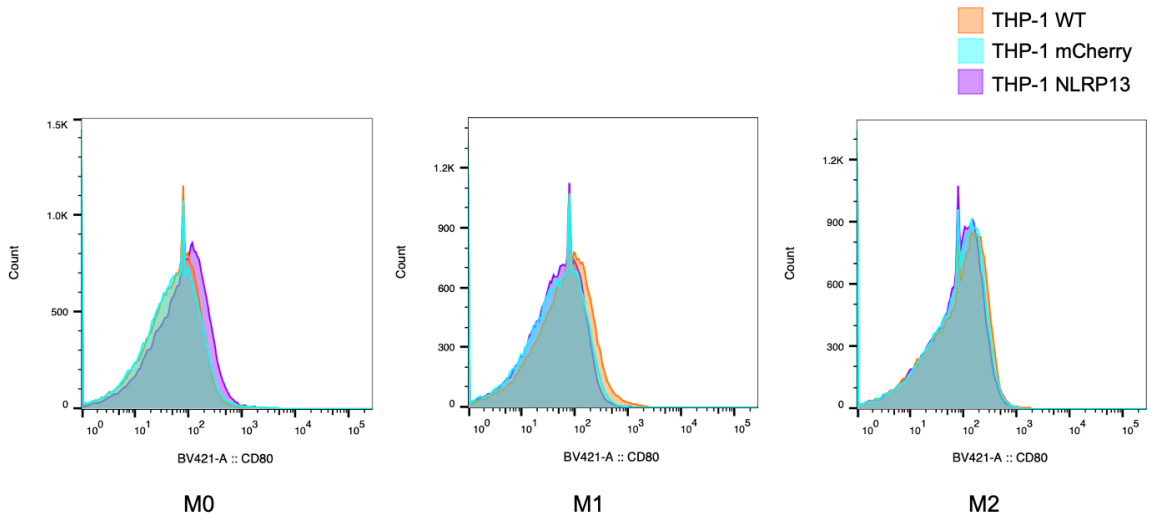


Figure 5.16. CD80 cell surface marker expression in monocytes, M0, M1 and M2 macrophages of WT, mCherry and NLRP13 THP1.

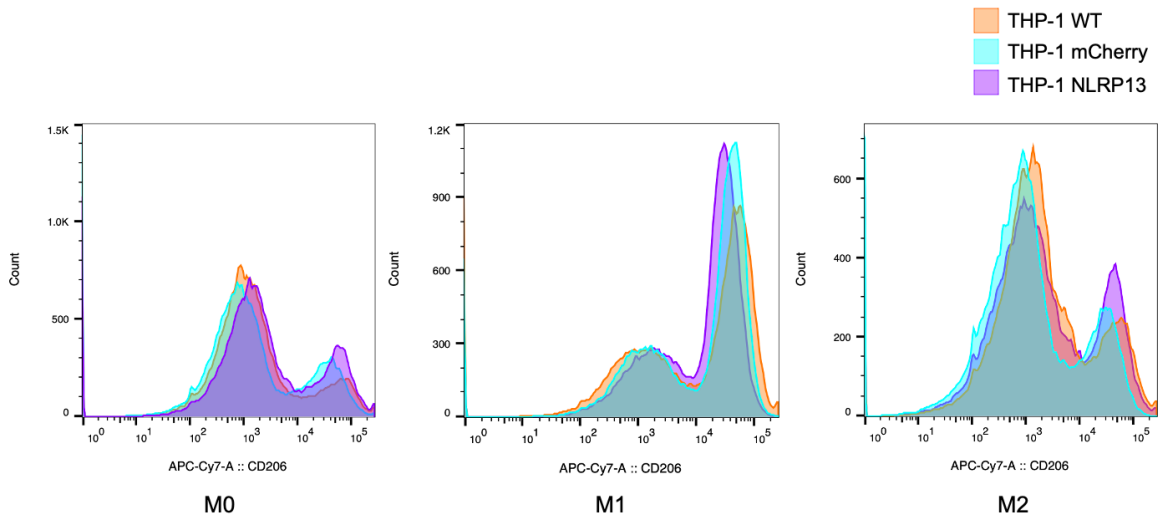


Figure 5.17. CD206 cell surface marker expression in monocytes, M0, M1 and M2 macrophages of WT, mCherry and NLRP13 THP1.

5.3. Knockdown of NLRP13 in THP-1 Cells via CRISPR/CAS9 Technology

For the knockdown of NLRP13, the dox inducible CRISPRi/Cas9 system was planned to be used.

Firstly, sgRNA-containing viruses were produced. To do so, 3 million HEK293FT cells were seeded to 10 cm^2 plates in a 10 mL medium the day before. The next day, they were transfected with envelope and packaging plasmids pVSVg, $\delta 8.2$ and sgRNA plasmids. Transfection efficiency was checked after 48 hours with fluorescence microscopy thanks to sgRNA plasmids containing GFP-tag (Figure 5.18). The sg groups, sg4 and sg5, which have none to very low transfection efficiency were eliminated. The medium of the cells was collected 48 hours later and directly used after filtering with 0.45 μm filters.

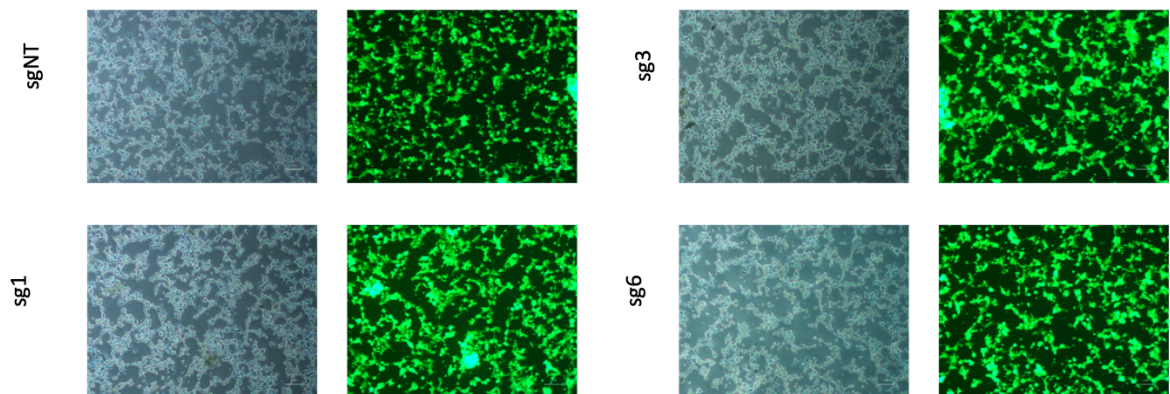


Figure 5.18. Transfection efficiency of HEK293FT cells transfected with sgRNA plasmids along with the packaging plasmids.

Dox-inducible Cas9 stable THP1 cells were seeded as 1 million/well to 6 well plates in 1 mL full RPMI medium. 1 ml of virus-containing medium was added on top of the cells. The cells were centrifuged for 90 minutes at 2900 rpm. The transduction efficiency was checked via flow cytometry after 72 hours: Transduction efficiency was found to be between 59-67.2% (Figure 5.19).

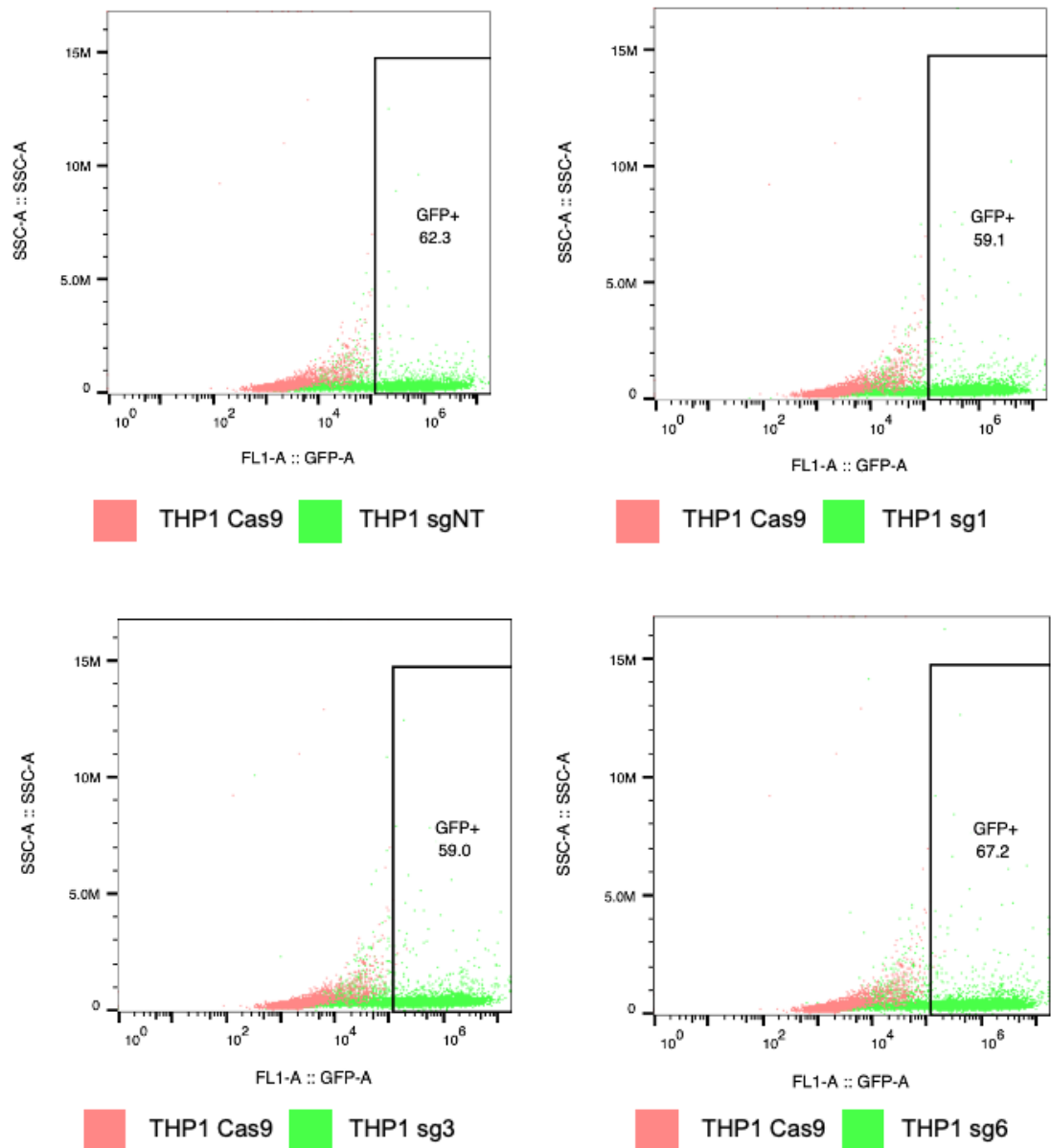


Figure 5.19. Transduction efficiency of lentiviral guide RNA containing viruses.

When they reach a sufficient number, the GFP-positive cells were sorted via Sony SH800 FACS and kept in 2x Pen-Strep containing full RPMI medium for 2 weeks. Then, they were selected for Cas9 positivity with 1 ug/ml puromycin for 2 weeks. After selection and sorting, the GFP positivity of the cells was increase up to 98.8% (Figure 5.20).

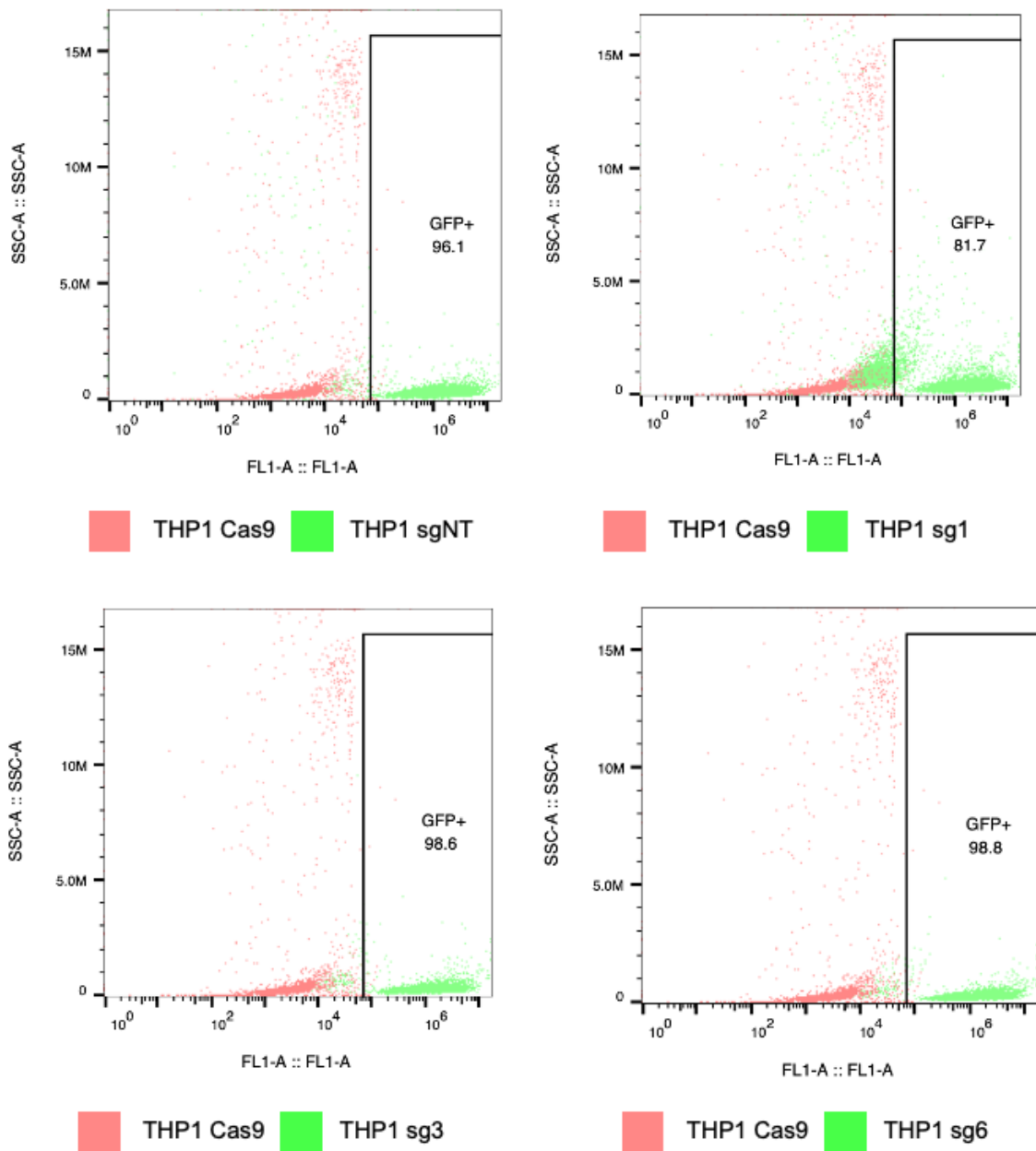


Figure 5.20. GFP Positivity after sorting according to GFP positivity and selecting via puromycin.

The cells were induced with 2 ug/ml doxycycline for 5 days. Cas9 is confirmed to be expressed upon dox induction in dox-inducible Cas9 stable cells (Figure 5.21). However, the endogenous NLRP13 protein and mRNA levels were too low to understand whether there is a successful knockdown in these cells via Western Blotting and RT-qPCR (Figure 5.22).

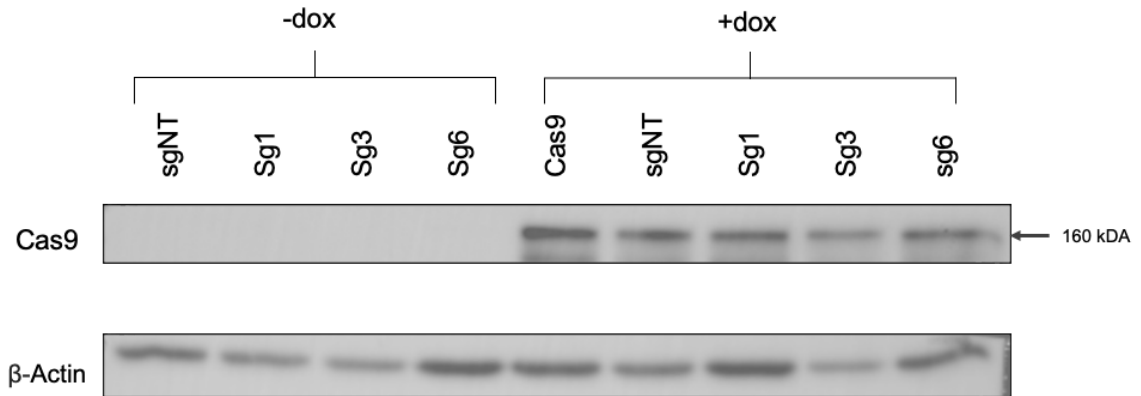


Figure 5.21. Protein expression of Cas9 upon dox induction.

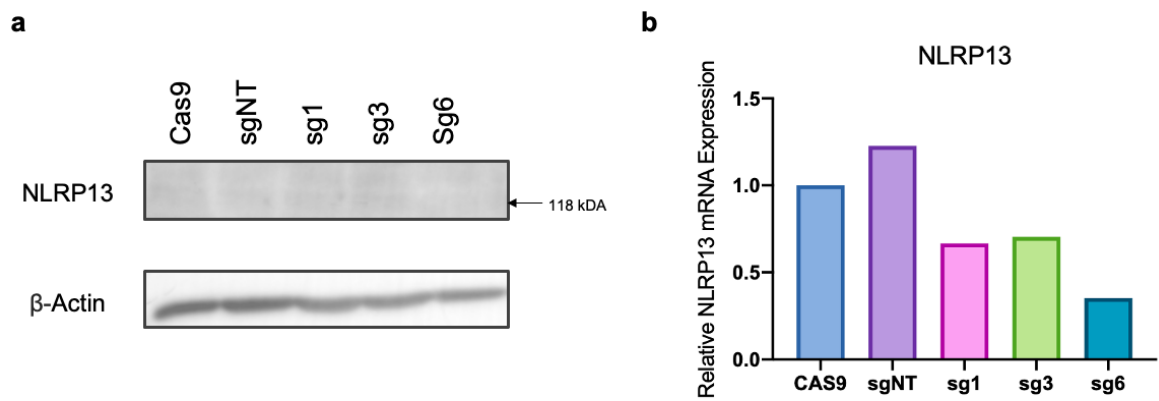


Figure 5.22. The expression of NLRP3 in guide RNA containing THP1 cells after dox induction. (a) The protein expression of NLRP3 (b) The relative mRNA expression of NLRP3.

Therefore, alternative strategies were attempted to determine the success of knockdown. The cells were treated with dox for 10 days, and genomic DNA samples were collected on days 0, 2, 4 and 7. The genomic DNA samples were amplified and sent to sequencing with primers designed to amplify the region containing locations

targeted by sgRNAs (Figure 5.23). On day 10, the cells were treated with 20 ng/ml PMA to be differentiated into macrophages in 3% FBS containing medium. Their medium was changed to complete medium the next day. After one day of rest, they were treated with 100 ng/ml LPS for 6 hours and 2 mM ATP for 30 minutes to induce the NLRP13 expression. There was no difference in protein expression of NLRP13 when it was compared to the control group, sgNT-containing cells (Figure 5.24). Also, sequencing results showed that there is no knockdown in these cells.

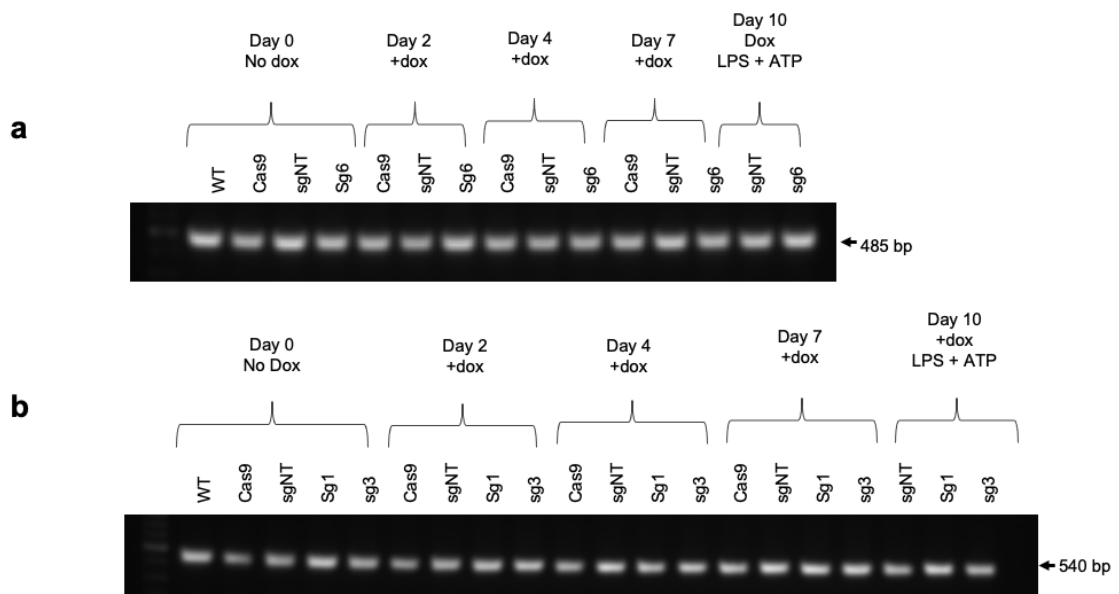


Figure 5.23. Agarose gel visualization of PCR amplification of the regions targeted by guide RNAs.

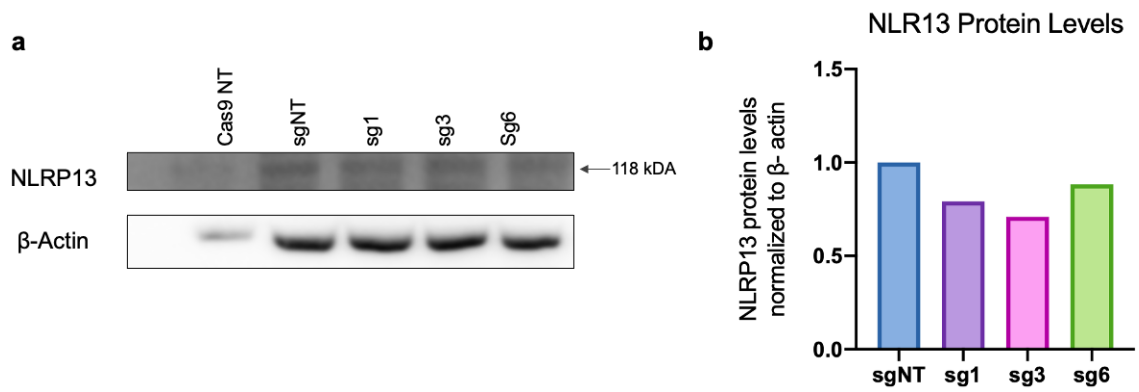


Figure 5.24. NLRP13 protein expression upon LPS/ATP treatment in guide RNA containing THP1 macrophages.

6. DISCUSSION

NLRP13 is a novel pyrin-containing NLR gene that can be found in humans, bovines, dogs, and chimpanzees but not in rodents. There is limited information in the literature about NLRP13. It is only mentioned in a few papers. These papers indicate that NLRP13, a maternal effect gene, might have roles in *Toxoplasma gondii* infection, doxorubicin resistance, and survival in HIV and tuberculosis coinfection. NLRP13 was studied by three former members of our laboratory. It was revealed that NLRP13 is localized in the cytosol and partly in mitochondria and also weakly interacts with inflammasome components (Gültekin, 2011). Its expression increases upon LPS/ATP treatment and *P. aeruginosa* infection (Yalçinkaya, 2015; Yilmazer, 2018). The pro-inflammatory response was shown to be enhanced with LPS/ATP treatment and *P. aeruginosa* infection in NLRP13 overexpressed THP1 cells compared to WT cells (Yilmazer, 2018). Additionally, NLRP13 overexpressed THP-1 macrophages exhibited a similar cytokine profile to M1 macrophages with higher levels of IL-6, IL-6Sr, IL-1 β , GM-CSF, TNF- α , and RANTES (CCL5) when compared to wild-type THP-1 (Yalçinkaya, 2015). It was also shown that NLRP13 is cleaved by Caspase-8 (Yilmazer, 2018). In this study, the localization of cleaved NLRP13 and its possible involvement in macrophage polarization was investigated.

Currently, there is no evidence of NLRs cleavage by caspases in the literature. The only NLR known to be cleaved NLRP1B in mice is activated upon cleavage by anthrax lethal toxin *B. anthracis* and forms inflammasome to initiate the downstream pro-inflammatory response. Human homolog, NLRP1, also has been shown to mimic the cleavage site of some viral proteases of the picornavirus family. It was also detected that there is more than one viral protease cleaving NLRP1B, too. Thus, it could be said that this variety in cleavage sites in NLRP1 stems from an evolutionary race between the virus and NLRP1 (Tsu, 2021). Even though the concept of cleavage differs at the point that NLRP13 is cleaved by an endogenous protease, Caspase-8, there still might be similarities in the sense of activation and regulation upon cleavage.

In this thesis, I focused on Caspase-8. Caspase-8 is a very versatile protease. Other than being the executioner caspase during cell death, it can also trigger the NF- κ B and promote the pro-IL1 β and NLRP3 expression (Gurung and Kanneganti, 2015). It was also recently found that Caspase-8 directly joins the NLRP1 inflammasome formation during SARS-CoV-2 infection (Planès, 2022). Considering these, the cleavage of NLRP13 by Caspase-8 is a unique and interesting topic to investigate.

To understand the cleavage of NLRP13 in the cells, we firstly aimed to determine the localization of its cleaved forms. To study the localization of cleaved NLRP13, an HA tag was added to the C-terminal of NLRP13 protein which already contains the FLAG sequence at the N-terminal using PCR integration. After this FLAG-NLRP13-HA sequence containing pcDNA3 plasmid was successfully obtained, it was transfected to HEK293FT cells along with the markers for mitochondria (MTS-DsRED), early endosomes (Rab5), late endosome to trans-Golgi network (Rab9), post-Golgi membranes (Rab11). The cells were treated with Fas Ligand CD95 antibody to bind Fas receptors on HEK293Ft cells and activate downstream endogenous Caspase-8 through Fas-Activated Death Domain (FADD). Immunofluorescence was performed with antibodies against FLAG and HA, and the samples were visualized with confocal microscopy. During the trial of CD95 treatment, it was seen that Caspase-8 is partly active, and NLRP13 was partially cleaved with no Fas Ligand. However, it was seen that colocalization is significantly increased with mitochondria and the C-terminal of NLRP13 after the CD95 treatment in comparison to untreated cells. It can be concluded that NLRP13 is cleaved by active Caspase-8, and the cleaved C-terminal is partly localized to mitochondria. It was also seen that NLRP13 does not participate in intracellular endosomal trafficking as there was no colocalization of FLAG and HA with Rab5, Rab9, or Rab11 with or without treatment.

Mitochondria play essential roles in the middle of immune response pathways of TLR, RLR, and NLR. A protein placed on the outer membrane called mitochondrial antiviral signaling protein, MAVS, triggers the secretion of pro-inflammatory cytokines and type-1 interferon as a part of the RLR signaling pathway (Andrieux, 2021). Additionally, NLRX1 is a mitochondrial targeting sequence containing NLR with a not

yet defined N-terminal domain X. NLRPX1 interacts with MAVS to prevent its binding RIG-I and thereby avert the downstream signaling of pro-inflammatory cytokines and IFN (Fekete, 2021). Also, cardiolipin and mitochondrial ROS activate the NLRP3 inflammasome (Andrieux, 2021). In their recent publication, Gebremicael *et al.* indicates the importance of NLRP13 in HIV and tuberculosis coinfection might suggest NLRP13's involvement in mitochondrial antiviral response.

NLRP13 does not include a mitochondrial localization signal. Thus, it is possible that it is carried by interaction with other proteins. For further study, caspase-8 inhibition could be included in the experimental set-ups, and cleaved NLRP13 localization might be checked with mitochondrial fractionation following caspase-8 activation. Even though the possible cleavage sites of NLRP13 were determined with a prediction tool, the exact cleavage site is not yet known. The estimated sites could be analyzed by site-directed mutagenesis and be identified. Later, the cleaved parts of NLRP13 could be separately overexpressed in different cell lines, and their possible roles in cytokine secretion or cell death could be studied.

It was shown that cytokine profiling of NLRP13 overexpressing THP-1 macrophages, biased towards M1 macrophages. It is also speculated that Caspase-8 might be involved in macrophage polarization, although the mechanism of which has not been enlightened yet. We hypothesized that NLRP13 might have a role in macrophage polarization with its cytokine profiling and Caspase-8 cleavage.

With the aim of determining whether NLRP13 may have a role during macrophage polarization, different subsets of macrophages, M0, M1, and M2, were examined in stably NLRP13 overexpressed THP1 cells versus control. The mRNA and surface expression levels of CD80 and CD206 markers were controlled. Even though a small increase in CD80 mRNA expression was observed, there were no differences in cell surface expression of each group. As a result, NLRP13 is not considered to have a function in macrophage polarization in THP1 macrophages. Although, different markers could be checked, such as CD86 (M1 marker), and CD163 (M2 marker). While a similar amount of NLRP13 protein levels were detected for M0, M1, and M2

macrophages in THP1 WT cells, different sizes of a band at approximately 130 kDa were noticed in THP1 monocytes with NLRP13 antibody (Figure 5.14). There might be a post-translational modification that is eliminated in macrophages. The possible post-translational modifications should be investigated.

The attempt to knock down NLRP13 was not successful, although it was ensured that cells contained Cas9 and guide-RNAs through selection and sorting, and it was confirmed that Cas9 is expressed upon dox treatment. This can be due to poor guide RNA selection or poor survival or fitness of knockdown. For future projects of NLRP13, It is essential to have NLRP13 knockdown/knockout cell lines to study its functions. Therefore, different strategies for gene knockdown, such as siRNA or shRNA can be tried.

Throughout this study, it was concluded that the N-terminal of NLRP13 stays in the cytosol and partial colocalization of mitochondria and C-terminal of NLRP13 increases upon cleavage by Caspase-8 which is activated upon FADD recruitment following Fas ligand binding to Fas receptor (Figure 6.1). Furthermore, NLRP13 overexpression does not lead to a difference in THP1 macrophages polarized into M1 and M2 subtypes.

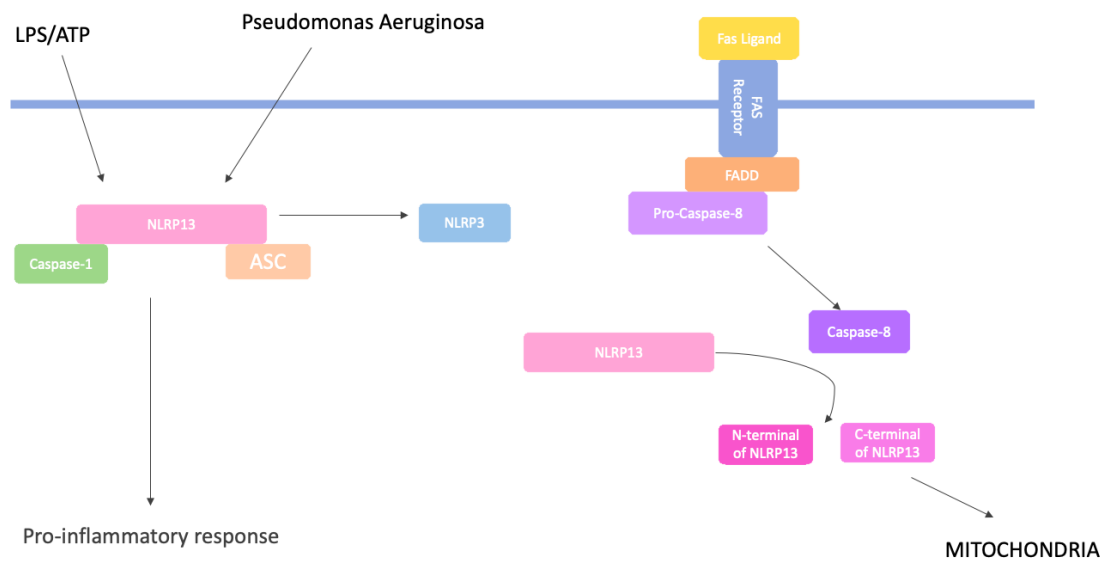


Figure 6.1. Updated model of NLRP3.

REFERENCES

- Alberts B., 2015, “Molecular Biology of the Cell.” 6th Edition, *Garland Science*, Taylor and Francis Group, New York.
- Andrieux P., C. Chevillard, E. Cunha-Neto, and J. P. S. Nunes, 2021, “Mitochondria as a Cellular Hub in Infection and Inflammation.” *International Journal of Molecular Sciences*, Vol. 22, Issue 21, p. 11338.
- Cuda C. M., A. v. Misharin, S. Khare, R. Saber, F. N. Tsai, A. M. Archer, P. J. Homan, G. K. Haines, J. Hutcheson, A. Dorfleutner, G. R. S. Budinger, C. Stehlik, and H. Perlman, 2015, “Conditional Deletion of Caspase-8 in Macrophages Alters Macrophage Activation in a RIPK-dependent Manner.” *Arthritis Research and Therapy*, Vol. 17, Issue 1, p. 291.
- Cullen S. P., and Martin S. J., 2009, “Caspase Activation Pathways: Some Recent Progress” *Cell Death and Differentiation*, Vol. 16, Issue 7, pp. 935–938.
- Deets K. A., and Vance R. E., 2021, “Inflammasomes and Adaptive Immune Responses.” *Nature Immunology*, Vol. 22, Issue 4, pp. 412–422.
- Fekete T., D. Bencze, E. Bíró, S. Benkő, and K. Pázmándi, 2021, “Focusing on The Cell Type Specific Regulatory Actions of NLRX1.” *International Journal of Molecular Sciences*, Vol. 22, Issue 3, pp. 1–36.
- Franchi L., N. Warner, K. Viani, and G. Nuñez, 2009, “Function of Nod-like Receptors in Microbial Recognition and Host Defense.” *Immunological Reviews*, Vol. 227, Issue 1, pp. 106–128.
- Gebremicael G., A. Gebreegziabxier, and D. Kassa, 2022, “Low transcriptomic of PT-PRCv1 and CD3E is an Independent Predictor of Mortality in HIV and Tuberculosis

Co-infected Patient.” *Scientific Reports*, Vol. 12, Issue 1, p. 10133.

Gültekin Y., 2011, *Cloning and Characterization of Novel Nod Like Receptors as Cytoplasmic Immune Sensors*, M.S. Thesis, Boğaziçi University.

Guo H., J. B. Callaway, and J. P. Y. Ting, 2015, “Inflammasomes: Mechanism of Action, Role in Disease, and Therapeutics.” *Nature Medicine*, Vol. 21, Issue 7, pp. 677–687.

Gurung P., and T. D. Kanneganti, 2015, “Novel Roles for Caspase-8 in IL-1 β and Inflammasome Regulation.” *American Journal of Pathology*, Vol. 185, Issue 1, pp. 17–25.

Han J. H., J. Park, T. B. Kang, and K. H. Lee, 2021, “Regulation of Caspase-8 Activity at the Crossroads of Pro-inflammation and Anti-inflammation.” *International Journal of Molecular Sciences*, Vol. 22, Issue 7, p. 3318.

Han J., Y. Jun, S. H. Kim, H. H. Hoang, Y. Jung, S. Kim, J. Kim, R. H. Austin, S. Lee, and S. Park, 2016, “Rapid Emergence and Mechanisms of Resistance by U87 Glioblastoma Cells to Doxorubicin in an *in vitro* Tumor Microfluidic Ecology.” *Proceedings of the National Academy of Sciences of the United States of America*, Vol. 113, Issue 50, pp. 14283–14288.

Kesavardhana S., R. K. S. Malireddi, and T. D. Kanneganti, 2020, “Caspases in Cell Death, Inflammation, and Pyroptosis.” *Annual Review of Immunology*, Vol. 38, Issue 1, pp. 567–595.

Kim Y. K., J. S. Shin, and M. H. Nahm, 2016, “NOD-like Receptors in Infection, Immunity, and Diseases.” *Yonsei Medical Journal*, Vol. 57, Issue 1, pp. 5–14.

Kostova I., R. Mandal, S. Becker, and K. Strebhardt, 2021, “The Role of Caspase-8 in the Tumor Microenvironment of Ovarian Cancer.”, *Cancer Metastasis Reviews*,

Vol. 40, Issue 1, pp. 303-318.

Li D., and Wu M., 2021., “Pattern Recognition Receptors in Health and Diseases.” *Signal Transduction and Targeted Therapy*, Vol. 6, Issue 1, p. 291.

Liu P., Z. Lu, L. Liu, R. Li, Z. Liang, M. Shen, H. Xu, D. Ren, M. Ji, S. Yuan, D. Shang, Y. Zhang, H. Liu, and Z. Tu, 2019, “NOD-like Receptor Signaling in Inflammation-associated Cancers: From Functions to Targeted Therapies.” *Phytomedicine*, Vol. 64, Issue 1, p. 152925.

Mandal R., J. C. Barrón, I. Kostova, S. Becker, and K. Strebhardt, 2020, “Caspase-8: The Double-edged Sword.” *Biochimica et Biophysica Acta - Reviews on Cancer*, Vol. 1873, Issue 2, p. 188357.

Planès R., M. Pinilla, K. Santoni, A. Hessel, C. Passemar, K. Lay, P. Paillette, A.-L. C. Valadão, K. S. Robinson, P. Bastard, N. Lam, R. Fadrique, I. Rossi, D. Pericat, S. Bagayoko, S. A. Leon-Icaza, Y. Rombouts, E. Perouzel, M. Tiraby, E. Meunier, 2022, “Human NLRP1 is a Sensor of Pathogenic Coronavirus 3CL Proteases in Lung Epithelial Cells.” *Molecular Cell.*, Vol. 82, Issue 13, pp. 2385–2400.

Platnich J. M., and D. A. Muruve, 2019, “NOD-like Receptors and Inflammasomes: A Review of Their Canonical and Non-canonical Signaling Pathways.” *Archives of Biochemistry and Biophysics*, Vol. 670, Issue 1, pp. 4–14.

Raggi F., S. Pelassa, D. Pierobon, F. Penco, M. Gattorno, F. Novelli, A. Eva, L. Varesio, M. Giovarelli, and M. C. Bosco, 2017, “Regulation of Human Macrophage M1-M2 Polarization Balance by Hypoxia and the Triggering Receptor Expressed on Myeloid Cells-1.” *Frontiers in Immunology*, Vol. 18, Issue 1, p. 1097.

Shalini S., L. Dorstyn, S. Dawar, and S. Kumar, 2015, “Old, New and Emerging Functions of Caspases.” *In Cell Death and Differentiation*, Vol. 22, Issue 4, pp. 526–539.

- Shapouri-Moghaddam A., S. Mohammadian, H. Vazini, M. Taghadosi, S. A. Esmaeili, F. Mardani, B. Seifi, A. Mohammadi, J. T. Afshari, and A. Sahebkar, 2018, “Macrophage Plasticity, Polarization, and Function in Health and Disease.” *Journal of Cellular Physiology*, Vol. 233, Issue 9, pp. 6425–6440.
- Shi C., and Pamer E. G., 2011, “Monocyte Recruitment During Infection and Inflammation.” *Nature Reviews Immunology*, Vol. 11, Issue 11, pp. 762–774.
- Strowig T., J. Henao-Mejia, E. Elinav, and R. Flavell, 2012, “Inflammasomes in Health and Disease.” *Nature*, Vol. 481, Issue 7381, pp. 278–286.
- Ting J. P. Y., R. C. Lovering, E. S. Alnemri, J. Bertin, J. M. Boss, B. K. Davis, R. A. Flavell, S. E. Girardin, A. Godzik, J. A. Harton, H. M. Hoffman, J. P. Hugot, N. Inohara, A. MacKenzie, L. J. Maltais, G. Nunez, Y. Ogura, L. A. Otten, D. Philpott, P. A. Ward, 2008, “The NLR Gene Family: A Standard Nomenclature.” *Immunity*, Vol. 28, Issue 3, pp. 285–287.
- Tsu B. v., C. Beierschmitt, A. P. Ryan, R. Agarwal, P. S. Mitchell, and M. D. Daugherty, 2021, “Diverse Viral Proteases Activate the NLRP1 Inflammasome.” *E-Life*, Vol. 10, Issue 1, p. 60609.
- van Oudenbosch N., and Lamkanfi M., 2019, “Caspases in Cell Death, Inflammation, and Disease.” *Immunity*, Vol. 50, Issue 6, pp. 1352–1364.
- Vanaja S. K., V. A. K. Rathinam, and K. A. Fitzgerald, 2015, “Mechanisms of Inflammasome Activation: Recent Advances and Novel Insights.” *Trends in Cell Biology*, Vol. 25, Issue 5, pp. 308–315.
- Wang S., Z. Wang, Y. Gu, Z. Li, Z. Li, F. Wei, and Q. Liu, 2016, “*Toxoplasma Gondii* Mitogen-Activated Protein Kinases are Associated With Inflammasome Activation in Infected Mice.” *Microbes and Infection*, Vol. 18, Issue 11, pp. 696–700.

- Yalçınkaya M., 2015, *Characterization of NLRP13 in Inflammasome Activity*, M.S. Thesis, Boğaziçi University.
- Yilmazer A., 2018, *Investigation of NLRP13-Driven Innate Immune Responses*, M.S. Thesis, Boğaziçi University.
- Yunna C., H. Mengru, W. Lei, and C. Weidong, 2020, “Macrophage M1/M2 Polarization.” *European Journal of Pharmacology*, Vol. 877, Issue 1, p. 173090.
- Zhang P., M. Dixon, M. Zucchelli, F. Hambiliki, L. Levkov, O. Hovatta, and J. Kere, 2008, “Expression Analysis of The NLRP Gene Family Suggests a Role in Human Preimplantation Development.” *PLoS ONE*, Vol. 3, Issue 7, p. 2755.
- Zheng D., T. Liwinski, and E. Elinav, 2020, “Inflammasome Activation and Regulation: Toward a Better Understanding of Complex Mechanisms.” *Cell Discovery*, Vol. 6, Issue 1, p. 36.
- Zhong Y., A. Kinio, and M. Saleh, 2013, “Functions of NOD-Like Receptors in Human Diseases.” *Frontiers in Immunology*, Vol 4, Issue 1, p. 333.

APPENDIX A: PLASMID MAPS

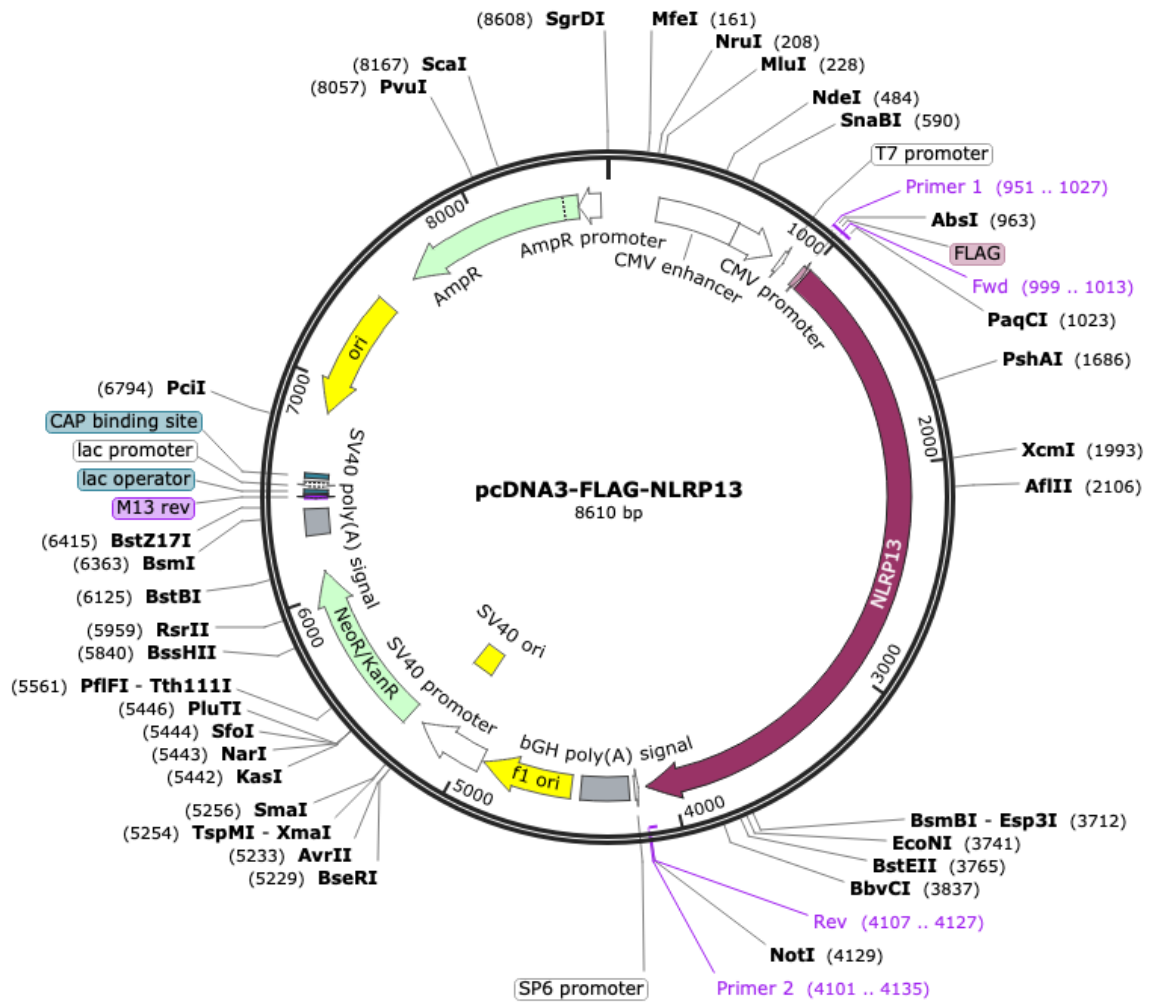


Figure A.1. Map of pcDNA3-NLRP13-FLAG vector.

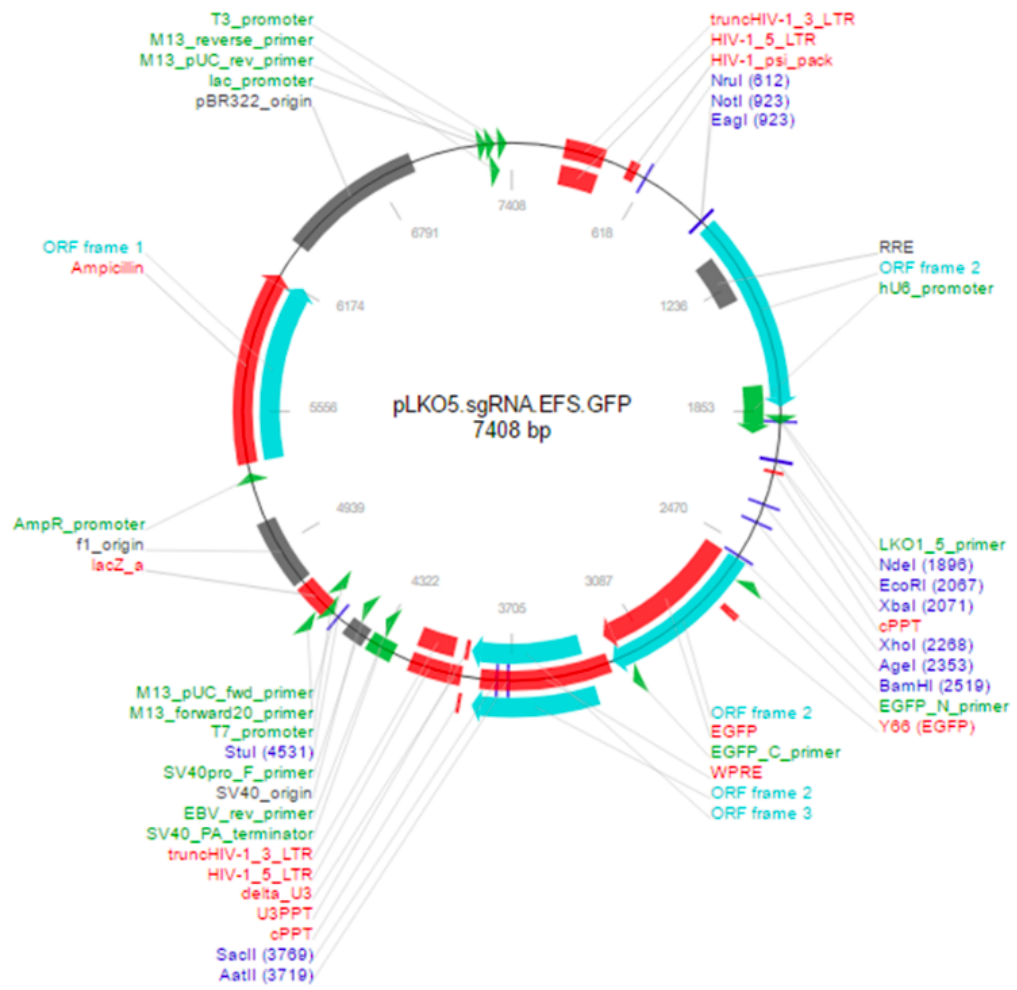


Figure A.2. Map of the pLKO5.sgRNA.EFS.GFP vector.